

CORROSION BEHAVIORS OF STAINLESS STEELS IN MOLTEN ZINC  
ALUMINUM ALLOY

A THESIS SUBMITTED TO  
THE GRADUATE SCHOOL OF NATURAL AND APPLIED SCIENCES  
OF  
MIDDLE EAST TECHNICAL UNIVERSITY

BY

EMRE ÖZCAN

IN PARTIAL FULFILLMENT OF THE REQUIREMENTS  
FOR  
THE DEGREE OF MASTER OF SCIENCE  
IN  
METALLURGICAL AND MATERIALS ENGINEERING

JULY 2012

Approval of the thesis:

**CORROSION BEHAVIORS OF STAINLESS STEELS IN MOLTEN ZINC  
ALUMINUM ALLOY**

submitted by **EMRE ÖZCAN** in partial fulfillment of the requirements for the degree of **Master of Science in Metallurgical and Materials Engineering Department, Middle East Technical University** by,

Prof. Dr. Canan ÖZGEN  
Dean, Graduate School of **Natural and Applied Sciences**

\_\_\_\_\_

Prof. Dr. C. Hakan GÜR  
Head of Department, **Metallurgical and Materials Engineering**

\_\_\_\_\_

Prof. Dr. Naci SEVİNÇ  
Supervisor, **Metallurgical and Materials Eng. Dept., METU**

\_\_\_\_\_

**Examining Committee Members:**

Prof. Dr. Tayfur ÖZTÜRK  
Department of Metallurgical and Materials Engineering, METU

\_\_\_\_\_

Prof. Dr. Naci SEVİNÇ  
Department of Metallurgical and Materials Engineering, METU

\_\_\_\_\_

Prof. Dr. İshak KARAKAYA  
Department of Metallurgical and Materials Engineering, METU

\_\_\_\_\_

Assoc. Prof. Dr. Arcan DERİCİOĞLU  
Department of Metallurgical and Materials Engineering, METU

\_\_\_\_\_

Dr. Abdi AYDOĞDU  
General Directorate of Mineral Research and Exploration

\_\_\_\_\_

**Date: 25.07.2012**

**I hereby declare that all information in this document has been obtained and presented in accordance with academic rules and ethical conduct. I also declare that, as required by these rules and conduct, I have fully cited and referenced all material and results that are not original to this work.**

Name, Last name: Emre ÖZCAN

Signature:

## **ABSTRACT**

# **CORROSION BEHAVIORS OF STAINLESS STEELS IN MOLTEN ZINC ALUMINUM ALLOY**

ÖZCAN, Emre

M. Sc., Department of Metallurgical and Materials Engineering

Supervisor: Prof. Dr. Naci SEVİNÇ

June 2012, 88 pages

High grade galvanized steel in large amounts is needed to match the increasing demand of automotive industry both in our country and in the world. Stainless steels, used in fabrication of zinc bath hardware of continuous galvanizing lines, lose their corrosion resistance due to various mechanisms in such mediums containing molten metals like zinc and aluminum. Consequently they corrode to the levels where they should be taken to maintenance or replaced. In this study, corrosion performance and the effect of typical galvanizing and age treating heat treatments to mechanical properties of 4 newly developed austenitic stainless steels and AISI 316L grade stainless steel were investigated and compared with each other. Experimental studies involved immersion corrosion tests for 168 and 504 hours followed by weight loss determinations and comparisons of corrosion performances of age treated and solution annealed stainless steels. Parallel with corrosion testing, delta ferrite content

determinations with 3 different methods, tensile tests and v-notch impact tests at 4 different heat exposure conditions were carried out and discussed. 2 new stainless steel compositions were selected to be used in fabrication of galvanizing hardware based on the comparisons of corrosion & mechanical performances of candidate steels.

Keywords: Stainless Steel, galvanize, molten metal corrosion, microstructure, mechanical properties.

## ÖZ

# PASLANMAZ ÇELİKLERİN ERGİMİŞ ÇİNKO-ALÜMİNYUM ALAŞIMI İÇİNDEKİ KOROZYON DAVRANIMLARI

ÖZCAN, Emre

Yüksek Lisans, Metalurji ve Malzeme Mühendisliği Bölümü

Tez Yöneticisi: Prof. Dr. Naci SEVİNÇ

Temmuz 2012, 88 sayfa

Dünyada ve ülkemizde, otomotiv sektöründeki artan talebin karşılanması için yüksek kalitede ve miktarda galvanizlenmiş çeliğe ihtiyaç duyulmaktadır. Sürekli Galvanizleme sürecinde, galvaniz kaplanacak çelik sacı galvaniz banyosunun içinden geçirmek için kullanılan paslanmaz çelikler, çinko, alüminyum gibi yüksek asitliğe sahip sıvı metallerin bulunduğu ortamlarda korozyon dayanımlarını çeşitli mekanizmaların etkinliğiyle kaybederler. Bunun sonucunda korozyona uğrayarak işlevlerini kaybedecek seviyede hasara uğrarlar ve önceden planlanmamış mekanik bakıma alınmaya veya değiştirilmeye ihtiyaç duyarlar. Bu çalışmada, 4 tane yeni geliştirilmiş östenitik paslanmaz çeliğin ve AISI 316L kalite paslanmaz çeliğin korozyon performansı ve sürekli galvanizleme sürecindeki tipik sıcaklık rejiminin bu paslanmaz çeliklerin mekanik özelliklerine etkisi araştırılmış ve birbirleri ile karşılaştırılmıştır. 5 aday çeliğe 168 saat ve 504 saatlik daldırma ile korozyon

deneyleri uygulanmış, takiben korozyona bağırlık kayıpları ölçülmüş ve birbirleri ile kıyaslamalar yapılmıştır. Yaşlandırılmış ve solüsyona alma tavlama yapılmış numuneler arasındaki korozyona bağırlık kayıpları karşılaştırılmıştır. Korozyon deneylerine paralel olarak aday çeliklere 3 farklı metot ile delta ferrit fazı tayini yapılmıştır. Mekanik deneylerde 4 farklı ısırl işlem sonrasında çekme ve v-çentik darbe deneyleri uygulanmış ve sonuçlar tartışılmıştır. Aday çelikler arasında, korozyon ve mekanik performansları göz önünde bulundurularak galvaniz potalarındaki donanımın üretiminde kullanılmak üzere 2 farklı paslanmaz çelik kompozisyonu seçilmiştir.

Anahtar Sözcükler: Paslanmaz çelik, galvaniz, korozyon, mikro yapı, mekanik özellikler

*To my dear family,*

## ACKNOWLEDGEMENTS

This thesis would not have been submitted without the help and contribution of several individuals who gave their valuable information and effort in the course of preparation and completion.

Firstly and most importantly, I would like to express my utmost gratitude to my supervisor dear Prof. Dr. Naci Sevinç for his great wisdom, patience and endless support during my thesis studies.

Secondly, I would like to present my special thanks to my employer Türker Gündüz, founder of Anadolu Metalurji ve Makine Sanayi Tic. A.Ş. for his moral and material support during my thesis studies. I would like to express my sincere gratitude to Kemal Cem Fadilloğlu, vice general manager of Anadolu Metalurji, for his great insights, guidance and valuable information throughout the entire study.

I would like to thank warmly to my colleagues Serkan Şahin and Mehmet Bozu who helped me with their valuable advises and efforts during experimental studies. I also would like to thank my friend Hakan Yavaş for all of his invaluable suggestions, comments and advises. Additionally, Assistant Prof. Dr. Caner Durucan, who allowed me to use his laboratory in the course of experimental works, is gratefully acknowledged.

Serkan Yılmaz, Research Associate of Metallurgical and Materials Engineering Department, is gratefully appreciated for his help and information regarding characterization of samples.

Members of examining committee of this M.Sc. thesis are specially acknowledged for their substantial comments, suggestions and time.

Last but not least, I cannot thank enough to my dear parents Masume Özcan and Önder Özcan whose encouragement have cleared the way for me to start and finish my thesis studies.

## TABLE OF CONTENTS

ABSTRACT .....	iv
ÖZ .....	vi
ACKNOWLEDGEMENTS .....	ix
TABLE OF CONTENTS .....	x
LIST OF FIGURES .....	xiii
LIST OF TABLES .....	xv

### CHAPTERS

1. INTRODUCTION .....	1
2. LITERATURE SURVEY .....	4
2.1. Past Studies Related Corrosion Performance Ranking .....	4
2.2. Stainless Steels .....	6
2.2.1. Austenitic Stainless Steels .....	8
2.2.2. Ferritic Stainless Steels .....	9
2.2.3. Martensitic Stainless Steels .....	10
2.2.4. Precipitation Hardening Stainless Steels .....	10
2.2.1. Duplex Stainless Steels .....	12
2.3. Continuous Galvanizing Lines and Coating Types .....	14
2.3.1. Galvanizing .....	15
2.3.2. Galvannealing .....	16
2.3.3. 55 % Aluminum – Zinc .....	18
2.3.4. Galfan <sup>®</sup> .....	19
2.3.5. Galvanizing Line Hardware .....	21
2.3.6. Sink Rolls .....	22

2.4. Galvanizing Metallurgy with Bath Hardware .....	24
2.4.1. Effect of Aluminum .....	24
2.4.2. Role of Delta Ferrite in Austenitic Stainless Steels .....	28
2.4.3. Control of Delta Ferrite in Austenitic Stainless Steels .....	29
2.4.3.1. Schaeffler & Delong Diagrams .....	30
2.4.3.2. Schoefer&WRC 1992 Diagrams.....	32
2.4.3.3. ORNL Diagram .....	35
2.4.3.4. Feritscope <sup>®</sup> .....	36
2.4.3.5. Metallographic Methods .....	37
2.5. Thermally Induced Embrittlement .....	37
2.5.1. Sensitization.....	38
2.5.2. 475 °C Embrittlement .....	40
2.5.3. Sigma Phase Embrittlement.....	41
3. EXPERIMENTAL PROCEDURE .....	44
3.1. Sample Production of Candidate Steels .....	44
3.2. Delta Ferrite Determination.....	45
3.3. Corrosion Testing .....	47
3.3.1. Corrosion Specimen Preparation .....	47
3.3.2. Immersion Corrosion Tests.....	48
3.3.3. Pickling of Coatings.....	51
3.3.4. Corrosion Damage Evaluation.....	52
3.4. Mechanical Tests .....	53
3.4.1. Sample Preparation and Heat Treatment .....	53
3.4.2. Tensile & Charpy Impact Tests .....	55
3.5. Scanning Electron Microscopy (SEM) Characterization of Galvanizing Bath.....	56
4. RESULTS AND DISCUSSION .....	58
4.1. Delta Ferrite Determination.....	59
4.2. Characterization of Galvanizing Bath .....	62
4.3. Immersion Corrosion Test Results & Corrosion Rates .....	66
4.4. Mechanical Testing Results.....	72
4.4.1. Steel 1 .....	72

4.4.2. Steel 2 .....	73
4.4.3. Steel 3 .....	74
4.4.4. Steel 4 (AISI 316L).....	75
4.4.5. Steel 5 .....	76
4.4.6. Discussion of Mechanical Testing Results .....	76
5. CONCLUSIONS.....	80
REFERENCES.....	83

## LIST OF FIGURES

### FIGURES

Figure 2.1 Ranking of candidate alloys after static corrosion test for 500 hrs. at 465 °C [7, 8].	5
Figure 2.2 Summary of stainless steel family [12].	7
Figure 2.3 SEM image of a cross sectioned steel sample after galvanizing [20].	15
Figure 2.4 Phase formation stages of galvanneal coating [21].	17
Figure 2.5 SEM image of Galvalume <sup>®</sup> coating taken from the cross-section of a steel sample [21].	19
Figure 2.6 Microstructure of Galfan <sup>®</sup> coating showing lamellar structure [27].	20
Figure 2.7 Overall picture of a continuous galvanizing line [29].	22
Figure 2.8 Schematic view of galvanizing bath showing function of galvanizing hardware.	23
Figure 2.9 Cross sectioned image of a galvanizing bath containing aluminum showing ternary Fe-Al-Zn alloy [32].	25
Figure 2.10 Corrosion rate of the AISI 316L stainless steel depending on the Al concentration in galvanizing bath at 500 °C [2].	26
Figure 2.11 Zinc-rich part of the Zn-Fe-Al phase diagram at 500 °C [35].	27
Figure 2.12 Optical Microscope Image of 316L Stainless Steel showing delta ferrite phase (dark regions) [39].	29
Figure 2.13 Schaeffler's constitution diagram [41].	31
Figure 2.14 DeLong's constitution diagram [43].	32
Figure 2.15 Schoefer's Diagram for predicting delta ferrite volume percent [44].	33
Figure 2.16 WRC-1992 diagram [46].	34
Figure 2.17 Modified version of Schaeffler's Diagram by ORNL with original Schaeffler's diagram.	35

Figure 2.18 Chromium depletion due to the carbide precipitation at the grain boundaries of steel [56].	39
Figure 2.19 Micrographs of the weld decay caused by intergranular corrosion of stainless steel [57].	39
Figure 3.1 Candidate steels in form of tubes.	45
Figure 3.2 Feritscope <sup>®</sup> FMP30.	46
Figure 3.3 Immersion Corrosion Test Specimens.	48
Figure 3.4 Melting Furnace.	49
Figure 3.5 Photograph of corrosion specimens to the molten zinc-aluminum alloy hooked up with wires.	50
Figure 3.6 Photo of mechanical test specimens as cut from rings.	53
Figure 3.7 Heat treatment of rough machined mechanical test specimens in annealing furnace.	54
Figure 3.8 Tensile testing device	55
Figure 3.9 Impact Testing Machine	56
Figure 3.10 SEM used for microstructural characterization	57
Figure 4.1 Metallographic image analysis result of AND-5 Steel.	60
Figure 4.2 Delta ferrite estimation of Steel 4 and 5 according to ORNL Diagram ...	61
Figure 4.3 Cross sectioned SEM image of galvanize coating (BS).	63
Figure 4.4 EDS analysis pattern for stainless steel – coating interface where $Fe_2Al_5$ - $_xZn_x$ formation is observed.	63
Figure 4.5 EDS analysis pattern for outer layer of stainless steel – coating.	65
Figure 4.6 Corrosion tested condition of specimens 4A (black one) and 5A.	71

## LIST OF TABLES

### TABLES

Table 2.1 Application fields of stainless steels [10].	8
Table 2.2 Chemical compositions of precipitation hardening stainless steels [10].	11
Table 2.3 Chemical compositions of duplex stainless steels [10].	13
Table 2.4 Properties of Phases of alloy layers in galvanizing [20].	16
Table 2.5 Phase distribution and chemical compositions in galvanized coating [21].	17
Table 2.6 Comparison of Galfan <sup>®</sup> with other types of coatings [27].	21
Table 2.7 Aluminum contents of different types of coatings [18, 34].	27
Table 3.1 Chemical Compositions of five candidate steels tested in this study	44
Table 3.2 Corrosion test conditions	51
Table 3.3 Heat treatment conditions and time intervals.	54
Table 4.1 Delta Ferrite Measurement Results with Feritscope <sup>®</sup>	59
Table 4.2 Typical chemical composition of galvanizing bath.	62
Table 4.3 Chemical composition of eta ( $\eta$ ) phase in atomic and weight percent.	64
Table 4.4 Chemical compositions of outer layer of coating in atomic and weight percent.	65
Table 4.5 Mass loss values of corrosion specimens.	67
Table 4.6 Weight loss comparison at different time intervals.	68
Table 4.7 Corrosion rates & mass loss per unit area values for corrosion specimens	69
Table 4.8 Mechanical tests results of steel 1	73
Table 4.9 Mechanical tests results of steel 2	73
Table 4.10 Mechanical tests results of steel 3	74

Table 4.11 Mechanical tests results of AISI 316L.....	75
Table 4.12 Mechanical tests results of AISI 316L.....	76
Table 4.13 Equivalent Chromium Contents of 5 Candidate Steels.....	78

# CHAPTER 1

## INTRODUCTION

Automobile panels, bodies and various components in automotive industry; cabinet doors, main surfaces of refrigerator and dishwashers etc. in white goods industry are the major fields which need enormous amounts of galvanized steel sheets. Increase on demand of galvanized steel sheet of these two industries have brought quality and efficiency problems with it.

Based on the information on “World Directory: Continuous Galvanizing Lines 2010”, there are over 450 continuous galvanizing lines where the coating of steel sheet with liquid zinc-aluminum alloy is carried out across the world. In United States, 25 companies have annual galvanizing capacity of approximately 19.940.000 metric tons in 61 continuous galvanizing lines. Annual galvanized steel sheet production of Turkey is approximately 2.700.000 metric tons in 9 galvanizing lines. Furthermore 3 new lines are in the stage of installation [1]. Even though the lifetime of the hardware used in zinc pots of continuous galvanizing lines have the most critical effect on line stoppages thus operating costs, very rare studies have been done focusing the development of more resistant and cost efficient materials instead of them until previous decade. Nowadays, engineers, scientists and technicians, working in continuous galvanizing lines, are being challenged to develop superior materials to replace existing ones since both customers and operators of galvanized steel strip industry are demanding even greater quality and efficiency [2].

In this study, corrosion behaviors of AISI 316L and 4 newly developed stainless steels in galvanizing media are investigated. Static immersion corrosion tests are conducted in a specific galvanizing medium containing 0.14 to 0.21 wt. % aluminum. Corrosion performances of candidate materials are evaluated with weight loss due to dissolution in galvanizing bath. Additionally, mechanical behaviors of these 5 candidate steels depending on 4 different heat exposure conditions are studied via tensile and charpy impact test results.

### **Description of Company Anadolu Metalurji and Scope of This Study**

Anadolu Metalurji ve Makina Sanayi Ticaret A.S. was established in 1987 in Ankara, Turkey as a steel construction & machining plant. Now the Company has 11000 m<sup>2</sup> indoor and 145000 m<sup>2</sup> outdoor areas with the manufacturing capacity of 8000 tons of high quality steel. Some of major production capabilities of Anadolu Metalurji can be seen as follows:

- Precision turning and grinding of large diameters (cylindrical, conical or crown grinding)
- Cutting and precision boring of large pieces at Bohrwerk machines
- Axial boring up to 7 meters length
- Precision eccentric hole drilling up to 2.5 meters length on CNC controlled special Gun Drill Machine
- Surface Roughening of cylindrical pieces at Special Surface Roughening Machine at desired surface quality
- Strictly applied WPSs and PQRs: Welding of stainless steels, joint welding, hard facing and weld repairing of high carbon and high alloyed steels

Main products manufactured in Anadolu Metalurji are continuous caster equipment, hot rolling mill rolls, cold rolling mill rolls, molten metal transferring vehicles, power plant equipment (rotor rims and shafts), rings for rolling mill rolls, roll chocks and sink rolls and stabilizing rolls for continuous galvanizing lines.

As for production of sink rolls, Anadolu Metalurji not only manufactures these rolls from standard material grades such as AISI 316L, 310 etc. but also carries out its research & development projects in order to develop new materials specifically designated for continuous galvanizing lines. The scope of the current study is to develop new stainless steel compositions and specifications to be used as sink roll or stabilizing roll material in continuous galvanizing lines. It is aimed to increase the service life of sink rolls in comparison to most widely used materials in this application. On this manner, literature review of this study comprehends stainless steels, galvanizing and coating types, continuous galvanizing lines and critical features affecting service life of sink rolls in working conditions.

## **CHAPTER 2**

### **LITERATURE SURVEY**

#### **2.1. Past Studies Related Corrosion Performance Ranking**

There have been more than several studies which have investigated the corrosion behaviors of stainless steels and various materials in galvanizing baths with certain chemical compositions. Brunnock et al. [3, 4] have investigated the corrosion performance of several stainless steels in a galvanizing bath with 0.135 wt. % aluminum content. Results of their studies showed that austenitic stainless steel grades have better corrosion resistance than ferritic and martensitic steels in this galvanizing media. Additionally, WC – Based coatings enhance corrosion performance of the steels.

In another corrosion performance related study, Jing Xu et al. [5] investigated 3 common types of steels in galvanizing media at different temperatures and time intervals. They have conducted immersion corrosion experiments to AISI 410, AISI 316L and AISI 1015 steels at 3 different (465, 500 and 520 °C) temperatures for 96 to 408 hours. They have found out that increasing temperature makes the corrosive media more aggressive and dramatically affects the corrosion rates. As for the corrosion performance of different types of steels, 316L outperformed martensitic stainless steel AISI 410 while it showed better performance than AISI 1015 carbon steel.

In 2007, Zhang et al. [6] have conducted corrosion testing of 316L stainless steel in an actual continuous galvanizing line. They have welded samples to various parts of the galvanizing hardware and characterized the microstructures of samples after subjecting them to galvanizing process. Dross build up on the samples are characterized when formation of  $Fe_2Al_5Zn_x$  phase is observed with SEM and Metallographic methods. They have observed that the morphologies of dross build ups are nearly the same regardless of the locations of the samples.

Among relatively recent studies, Sikka et al. [7, 8] have proposed a ranking of various alloys including AISI 316L, Triballoy 800, D2 tool steel etc. based on their corrosion performance in terms of weight loss in galvanizing media.

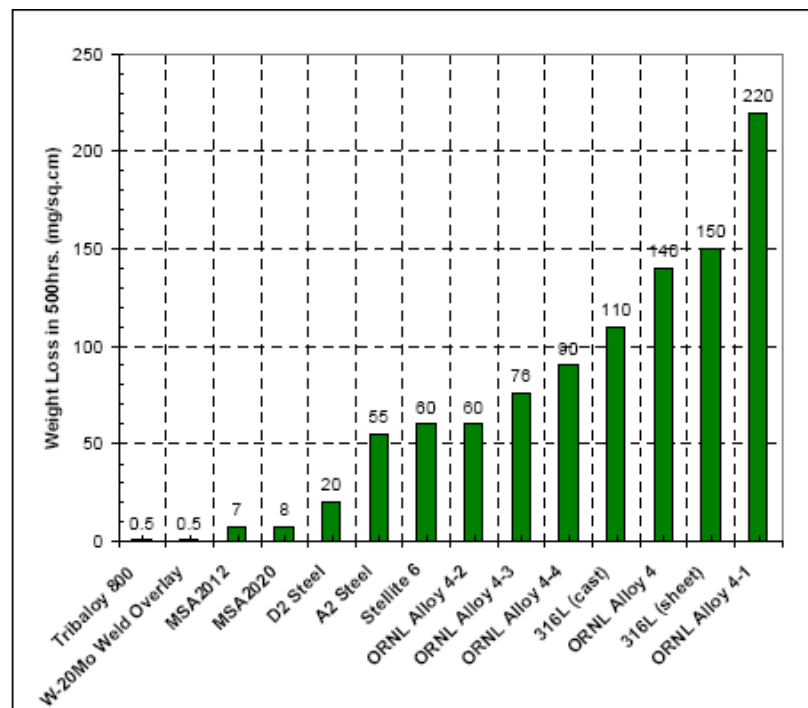


**Figure 2.1** Ranking of candidate alloys after static corrosion test for 500 hrs. at 465 °C [7, 8].

Figure 2.1 shows the weight loss of tested materials in Zinc – 0.16 wt. % Al galvanizing medium at 465 °C. In the proposed ranking, MSA 2012 and MSA 2020 produced by Metallurgical Systems Divisions of Pyrotek are ferrous superalloys with relatively rich amount of carbides, Triballoy 800, manufactured by Deloro-Stellite is a cobalt based superalloy and the alloy 4-x series of alloys, developed by Oak Ridge National Laboratory, are Fe-Cr-Al alloys. It is obvious that certain alloys showed extremely superior corrosion performance to common stainless steels but when it comes to the cost performance optimization for commercial usage of these alloys, AISI 316L is the most preferred material for heavy galvanizing bath hardware. It is not possible to use a sink roll which weighs approximately 2 metric tons from a relatively expensive superalloy [7, 8].

Actually, AISI 316L stainless steel is the most accepted and widely used material for galvanizing bath hardware such as sink rolls, stabilizing and correcting rolls. It is a high alloyed stainless steel containing significant amounts of Cr, Ni and a little of Mo and has very low carbon content (max 0.03 %). Addition of Cr makes this steel resistant to oxidation while Mo addition increases its pitting corrosion resistance. Addition of nickel not only makes it to have better toughness by maintaining austenitic structure at room temperature but also increases its corrosion resistance against neutral chloride solutions and other oxidizing acids [9].

## **2.2. Stainless Steels**

Stainless steels are iron-base alloys containing minimum of 11 % Chromium in order to prevent the rust formation in standard atmosphere conditions. They exhibit stainless property due to the formation of chromium-rich oxide surface film which heals itself continuously in the presence of oxygen. Other elements like carbon (ranging from less than 0.03 % to over 1.0 %) nickel, molybdenum, copper, titanium, aluminum, silicon, niobium, nitrogen, sulfur and selenium can be also present in their

structure to improve particular characteristics. Figure 2.2 shows the summary of stainless steel family [10, 11].

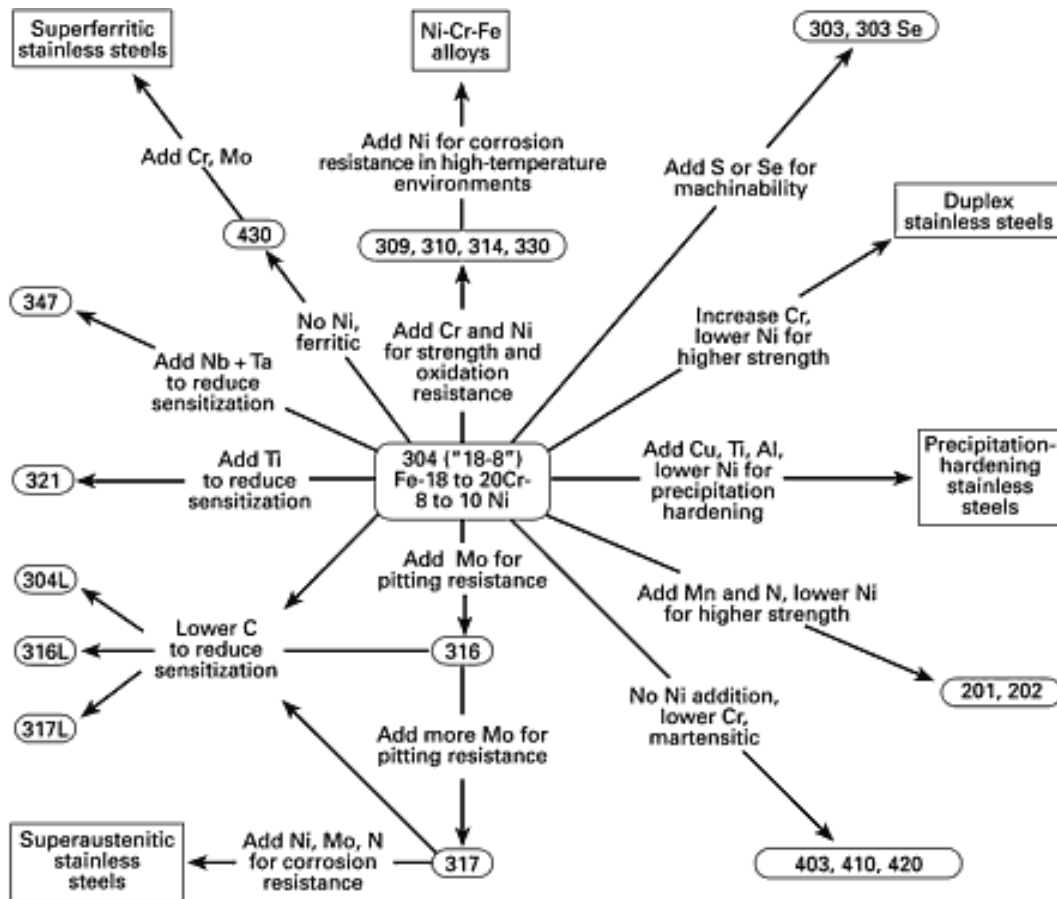


**Figure 2.2** Summary of stainless steel family [12].

As for the designation for stainless steels, American Iron and Steel Institute (AISI) uses the Unified Numbering system, or the name of the alloy. According to the classification of the AISI, 200 and 300 series are generally austenitic stainless steel grades while 400 series can either be ferritic or martensitic. The UNS system introduces 2 more digits and 1 letter “S” to the symbols of the stainless steels and so, it comprehends more (and also newly developed) stainless steels. Most of the UNS designation corresponds to an AISI number in its first three digits. If last two digits of the UNS number are different than zero, the number represents a grade other than basic AISI grade. For instance AISI 316 stainless steel is represented as S31600 in the UNS. As for the stainless steels containing higher nickel, in a range of 25 to 35

%, the UNS designation uses letter “N” followed by a five digit number. N08020 (20Cb3), N08024 (20Mo-4) and N08367 (AL-6XN) can be given as examples. Even though previously mentioned grades belong to nickel-base alloys according to the UNS, these examples constitute the “super-austenitic” category of stainless steels [10, 11]. Table 2.1 represents the application fields of stainless steels and classification of stainless steels are explained as follows:

**Table 2.1** Application fields of stainless steels [10].

<b>Application</b>	<b>Percentage</b>
<b>Industrial equipment</b>	
<b>Chemical and power engineering</b>	34
<b>Food and beverage industry</b>	18
<b>Transportation</b>	9
<b>Architecture</b>	5
<b>Consumer goods</b>	
<b>Domestic appliances, household utensils</b>	28
<b>Small electrical and electronic appliances</b>	6

### **2.2.1. Austenitic Stainless Steels**

Austenitic stainless steels are the largest group among stainless steels. They show non-magnetic characteristic in annealed condition and can be hardened only by cold working. Generally, they have great cryogenic properties and good high-temperature strength and oxidation resistance in atmosphere. As for their chemical compositions, they usually contain chromium in a range of 16 to 26 %, nickel up to 35 % and manganese up to 15 %. Other elements such as molybdenum, copper, silicon, aluminum, titanium, niobium, vanadium nitrogen etc. can be present at their structures in order to achieve various characteristics [10].

Mechanical properties of austenitic stainless steels depend on their alloying elements. Yield strength, tensile strength and elongations of 300 series steels in annealed condition are in a range of 205 – 275 MPa, 520 to 760 MPa and 40 to 60 % respectively. 200 series have better mechanical properties than 300 series. Their yield strengths range from 345 to 480 MPa and cold worked forms of 200 series alloys can have a tensile strength up to 1200 MPa or even higher [13].

All of the austenitic stainless steels have good corrosion resistance in standard atmospheric conditions, in most of the aqueous media and in oxidizing acids such as nitric acid. Various compositional modifications are applied to the stainless steels for enhancing the corrosion resistance of them for specific applications e.g., nitrogen is added to increase the strength and reduce the rate of chromium carbide precipitation and avoiding sensitization [13].

### **2.2.2. Ferritic Stainless Steels**

Ferritic stainless steels are iron-chromium alloys generally containing 11 to 30 % chromium with other alloying elements molybdenum, silicon, aluminum, titanium, niobium, selenium and low level carbon. They cannot be strengthened through heat treatment and have good ductility. Formability and weldability of these steels depends on the interstitial element content in their structure [10, 14].

Yield strengths of ferritic stainless steels range from 240 to 380 MPa while tensile strengths of these types of steels vary from 415 to 585 MPa. Their elongation levels are in a range of 20 to 35 %. Their corrosion resistance can be moderate or even higher based on their chromium contents. Low chromium containing ferritic stainless steels show moderate corrosion resistance whereas high chromium containing ones can show excellent corrosion properties. They usually exhibit weak high temperature

corrosion resistance and high temperature embrittlement due to the carbide formation in their microstructures [14, 15].

### **2.2.3. Martensitic Stainless Steels**

Martensitic stainless steels are high carbon containing iron-chromium steels with chromium contents of 10.5 to 18 % and carbon contents up to 1.2 %. They can be hardened via heat treatment and so they possess high mechanical performance. On the other hand, they show relatively low corrosion resistance compared to most of the ferritic and almost all of the austenitic stainless steels. Other elements like nickel, molybdenum, niobium, silicon, wolfram, vanadium, selenium can be alloyed in order to affect some particular characteristics such as machinability or toughness [10-12, 14].

Martensitic stainless steels have yield strength of about 275 MPa in their annealed conditions. However they can have yield strengths up to 1900 MPa based on their carbon levels after quenching and hardening [10, 15].

### **2.2.4. Precipitation Hardening Stainless Steels**

Precipitation hardening (PH) stainless steels are iron-chromium-nickel steels which can be hardened through aging [10]. Their micro structures can be adjusted with alloying elements, mainly with chromium, nickel and carbon. Phase distribution of these steels can be austenitic, semi-austenitic or martensitic. Alloying elements of PH series are generally titanium, aluminum, copper, niobium, some of which form precipitates and the other ones function as stabilizers [12, 14].

Similar with martensitic stainless steels, PH stainless steels can possess high yield strengths up to 1700 MPa and cold working before aging treatment can result even higher strengths. Besides these properties, PH series also have better ductility, toughness and corrosion resistance than martensitic stainless steels because of their balanced micro structures alloyed with high chromium, nickel, molybdenum and restricted carbon (max. 0.11) levels [15, 16]. Table 2.2 shows certain types of precipitation hardening stainless steels.

**Table 2.2** Chemical compositions of precipitation hardening stainless steels [10].

UNS No.	Alloy	Composition, %								
		C	Mn	Si	Cr	Ni	Mo	P	S	Other
<b>Martensitic types</b>										
<b>S13800</b>	PH13-8 Mo	0.05	0.10	0.10	12.25-13.25	7.5-8.5	2.0-2.5	0.01	0.008	0.90-1.35 Al; 0.01 N
<b>S15500</b>	15-5PH	0.07	1.00	1.00	14.0-15.5	3.5-5.5	...	0.04	0.03	2.5-4.5 Cu; 0.15-0.45 Nb
<b>S17400</b>	17-4PH	0.07	1.00	1.00	15.0-17.5	3.0-5.0	...	0.04	0.03	3.0-5.0 Cu; 0.15-0.45 Nb
<b>S45000</b>	Custom 450	0.05	1.00	1.00	14.0-16.0	5.0-7.0	0.5-1.0	0.03	0.03	1.25-1.75 Cu; 8 × %C min Nb
<b>S45500</b>	Custom 455	0.05	0.50	0.50	11.0-12.5	7.5-9.5	0.50	0.04	0.03	1.5-2.5 Cu; 0.8-1.4 Ti; 0.1-0.5 Nb
<b>Semiaustenitic types</b>										
<b>S15700</b>	PH15-7 Mo	0.09	1.00	1.00	14.0-16.0	6.50-7.75	2.0-3.0	0.04	0.04	0.75-1.50 Al
<b>S17700</b>	17-7PH	0.09	1.00	1.00	16.0-18.0	6.50-7.75	...	0.04	0.04	0.75-1.50 Al
<b>S35000</b>	AM-350	0.07-0.11	0.50-1.25	0.50	16.0-17.0	4.0-5.0	2.50-3.25	0.04	0.03	0.07-0.13 N
<b>S35500</b>	AM-355	0.10-0.15	0.50-1.25	0.50	15.0-16.0	4.0-5.0	2.50-3.25	0.04	0.03	0.07-0.13 N

**Table 2.2** Chemical compositions of precipitation hardening stainless steels  
(continued)

<b>Austenitic types</b>										
<b>S66286</b>	A-	0.08	2.00	1.00	13.5-	24.0-	1.0-	0.025	0.025	1.90-2.35 Ti; 0.35
	286				16.0	27.0	1.5			max Al; 0.10-0.50 V; 0.0030-0.0100 B
...	JBK-	0.015	0.05	0.02	14.5	29.5	1.25	0.006	0.002	2.15 Ti; 0.25 Al; 0.27
	75									V; 0.0015 B

### 2.2.1. Duplex Stainless Steels

Duplex stainless steels are iron-chromium-nickel alloys having a mixed microstructure of austenite and ferrite. They usually have approximately 50/50 austenite and ferrite based on their alloying contents. General chromium contents of duplex stainless steels are in a range of 20 to 30 % while nickel contents vary from 5 to 8 %. Carbon is restricted with 0.03 % maximum and these steels may also contain other alloying elements such as molybdenum, nitrogen, tungsten and copper. Their unique advantages over other stainless steels are higher strength in comparison with austenitic stainless steels and higher ductility levels in comparison with ferritic stainless steels [14-16].

Duplex stainless steels generally have yield strengths in a range of 550 to 690 MPa, which lets designers to reduce weight in critical applications such as pressure vessels. However, ferritic matrix of duplex stainless steels makes them brittle when they are exposed to elevated temperatures for extended periods. Therefore service temperature for these types of steels do not exceed 300 °C [15, 16]. Duplex stainless steels are widely used in oil and gas, petrochemical, pulp and paper industries. They are usually used instead of austenitic series since they have better corrosion resistance against chloride SCC or pitting [12, 17]. Chemical compositions of duplex stainless steels can be seen on table 2.3.

**Table 2.3** Chemical compositions of duplex stainless steels [10].

UNS number <sup>(a)</sup>	Type/designation	Composition <sup>(b)</sup> , %									
		C	Mn	S	P	Si	Cr	Ni	Mo	N <sub>2</sub>	Other
S31200/...	44LN	0.03	2.00	0.03	0.045	1.00	24.0-26.0	5.5-6.5	1.2-2.0	0.14-0.20	...
S31260/39226	...	0.03	1.00	0.030	0.030	0.75	24.0-26.0	5.5-7.5	2.5-3.5	0.10-0.30	0.10-0.50 W, 0.20-0.80 Cu
S31500/39215	...	0.03	1.2-2.0	0.03	0.03	1.4-2.0	18.0-19.0	4.25-5.25	2.5-3.0	0.05-0.10	...
S31803/39209	UR45N	0.03	2.00	0.02	0.03	1.00	21.0-23.0	4.5-6.5	2.5-3.5	0.08-0.20	...
S32304/39230	2304	0.03	2.5	0.04	0.04	1.0	21.5-24.5	3.0-5.5	0.05-0.60	0.05-0.20	0.05-0.60 Cu
S32550/39255	...	0.03	1.5	0.03	0.04	1.0	24.0-27.0	4.5-6.5	2.9-3.9	0.10-0.25	1.5-2.5 Cu
S32760/39276	Zeron 100	0.03	1.0	0.01	0.03	1.0	24.0-26.0	6.0-8.0	3.0-4.0	0.30	0.5-1.0 Cu, 0.5-1.0 W
S32900/...	Type 329	0.06	1.00	0.03	0.04	0.75	23.0-28.0	2.5-5.0	1.0-2.0	<sup>(b)</sup>	...
S32950/39295	7 Mo Plus	0.03	2.00	0.01	0.035	0.60	26.0-29.0	3.5-5.2	1.0-2.5	0.15-0.35	...

<sup>a</sup>Certain UNS numbers for duplex grades have been replaced. For example, S32950/39295 means that the original UNS No. (S32950) has been replaced by S39295.

<sup>b</sup>Not specified

### **2.3. Continuous Galvanizing Lines and Coating Types**

In simple terms, galvanizing is coating of steel by passing it through molten zinc. The word “Galvanize” comes from the galvanic protection since zinc is chemically more active than steel and it retains steel unoxidized when two of them are galvanically connected. Coated zinc also acts as a barrier and protects steel from corrosive agents [18].

Galvanizing is carried out in two different practices; one of which is general (batch) galvanizing and the other one is continuous galvanizing. In batch galvanizing, mostly finished products or near-finished products are coated and the practice is simple: cleaned products are immersed to the molten zinc bath and taken out. To the contrary, in continuous galvanizing, steel sheet is fed into the molten zinc bath steadily. The line speed (length of steel sheet fed into bath) of a continuous galvanizing line can be up to 183 meters per minute. When steel strip enter into the galvanizing bath, intermetallic compounds between steel and bath metals occur immediately. In general, coating thickness of steel strip, generally in terms of mass of coating per unit area, is controlled with gas-wipers [18].

First continuous galvanizing line has been established in Poland in 1936 [19]. Today, it is used by many manufacturers all over the world. Now it is also used to coat steel sheets with different metals or alloys such as aluminum or 55 % Aluminum – Zinc alloy. Early on continuous galvanizing, quality demands were not as high as it is today. Now automotive and white goods industries demand not only high surface quality but also good formability from the galvanized steel sheets [18].

### 2.3.1. Galvanizing

As mentioned in previous section, there are two ways for galvanizing the steel. Both ways involve dipping the steel in molten zinc bath. Melting point of zinc is 419 °C; therefore it must be heated above its melting point in order to provide proper bonding between steel and zinc. Usually zinc baths are heated to a temperature of approximately 460 °C and controlled at this temperature [20].

During continuous galvanizing, steel sheet interacts with the molten zinc in a range of 2 - 4 seconds before it exits the molten zinc bath. When it enters the zinc bath, intermetallic compounds between zinc and iron forms immediately and so intermetallic layers are generated on the steel surface. As shown in the figure 2.3, different phases are formed during galvanizing. Outer layer of the coating, eta phase, comprises of almost pure zinc and iron content of the coating increases as going towards bulk steel [20].

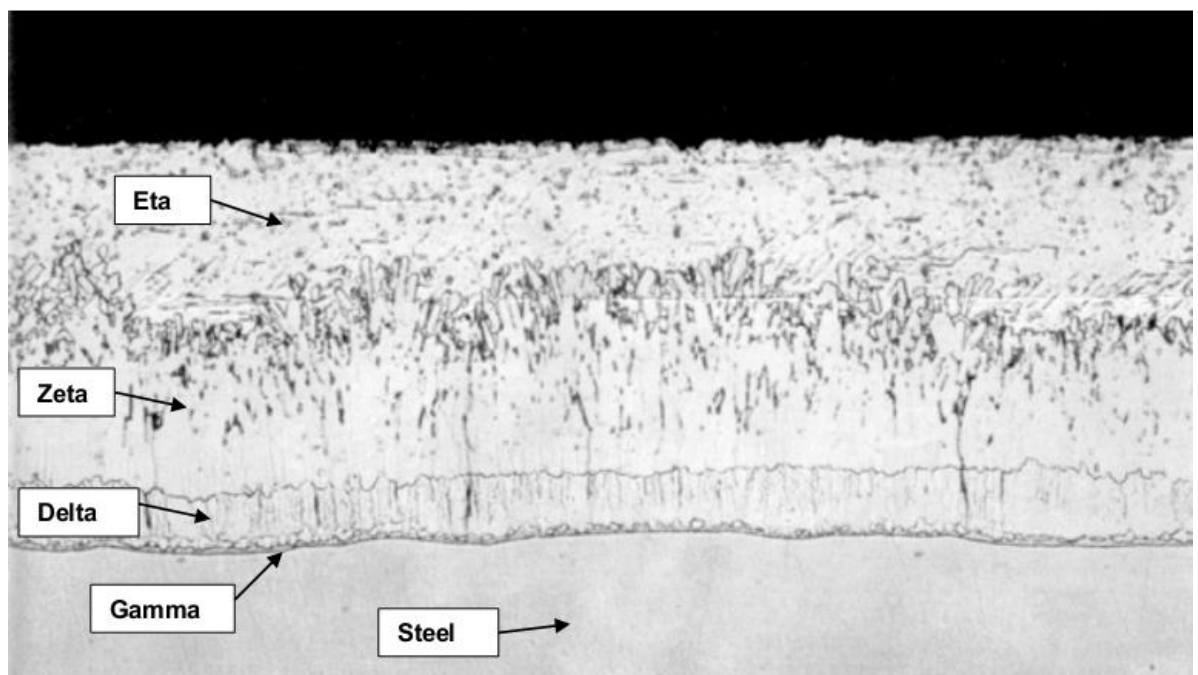


**Figure 2.3** SEM image of a cross sectioned steel sample after galvanizing [20].

As can be seen on the SEM image, almost 50 % of the thickness of the coating consists of two different Fe-Zn alloys. Each of these layers has different iron and zinc content and table 2.4 shows the approximate chemical compositions and other characteristics of the phases formed on the surface of the galvanized steel [20].

**Table 2.4** Properties of Phases of alloy layers in galvanizing [20].

<b>Layer</b>	<b>Alloy</b>	<b>Iron %</b>	<b>Melting Point (°C)</b>	<b>Crystal Structure</b>	<b>Mechanic Characteristics</b>
<b>Eta (<math>\eta</math>)</b>	Zinc	0,03	419	Hexagonal	Soft, ductile
<b>Zeta (<math>\zeta</math>)</b>	FeZn <sub>13</sub>	5,7 – 6,3	530	Monoclinic	Hard, brittle
<b>Delta (<math>\delta</math>)</b>	FeZn <sub>7</sub>	7,0 – 11,0	530 – 670	Hexagonal	Ductile
<b>Gama (<math>\gamma</math>)</b>	Fe <sub>3</sub> Zn <sub>10</sub>	20,0 – 27,0	670 - 780	Cubic	Hard, brittle
<b>Steel Base</b>	Iron - Carbon	>99	~ 1510	Cubic	Ductile

### 2.3.2. Galvannealing

In normal galvanizing, steel strip exits the galvanizing bath and excess zinc is wiped off with gas-wipers in order to obtain a uniform coating thickness. Galvannealing introduces one more step to this process. When steel passes the gas-wipers, it is fed into a heating furnace where it is heated to a temperature range of 500 - 565 °C with the purpose of changing the metallurgy of the coating. After steel is subjected to this treatment, iron content of zinc coating becomes 6 – 23 % (10 % in average) due to diffusion of iron through coating. Iron content in coating depends on diffusion rate, and hence on heat treatment temperature. Consequently there is no free zinc in galvanized coating so it has a mat appearance relative to galvanized coating [21].

Galvannealed coatings have approximately 9 - 12 % bulk iron along with some aluminum. Iron in galvannealed coating forms three different phases, which can be seen from table 2.5, with zinc. One of major differences between galvannealed and galvanized coating is aluminum content of molten metal bath which is discussed in sections 2.4 and 2.4.1.

**Table 2.5** Phase distribution and chemical compositions in galvannealed coating [21].

Phase	Iron %	Aluminum %
Zeta ( $\zeta$ ) FeZn <sub>13</sub>	5,2 – 6,1	0,7
Delta ( $\delta$ ) FeZn <sub>7</sub>	7,0 – 11,5	3,7
Gama ( $\gamma$ ) Fe <sub>3</sub> Zn <sub>10</sub>	15,8 – 27,7	1,4

Three phases which form during the heating stage of galvannealing compose in sequence. Firstly zeta phase forms and then goes to surface of coating by diffusion, then delta and gamma phases follow it respectively. Figure 2.4 shows phase formation stages of galvanneal.

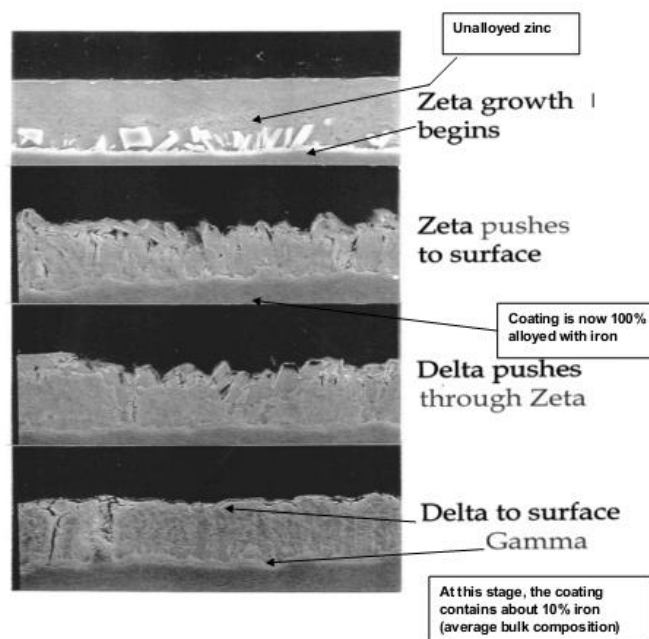


**Figure 2.4** Phase formation stages of galvanneal coating [21].

### 2.3.3. 55 % Aluminum – Zinc

Aluminum-Zinc coating was first introduced commercially by BIEC International Inc. in 1972 with a trade name called Galvalume<sup>®</sup> which is the most widely used name for this coating. It was originally developed in order to enhance corrosion resistance of the hot dip galvanized products [22, 23].

Molten metal bath of Galvalume<sup>®</sup> coating consists of 55 % Aluminum, 1.5 % silicon and 43.5 % zinc. Existence of silicon in coating bath is to inhibit the exothermic chemical reaction of aluminum and iron [24]. Therefore silicon is not added for enhancing corrosion performance but for restricting over formation of intermetallic alloy layer between bath metals and steel. During Galvalume<sup>®</sup> coating, an intermetallic alloy Fe-Zn-Al forms at the interface of bulk steel and coating [25]. The formability of Galvalume<sup>®</sup> coated sheets is not as good as that of galvanized sheet. For this reason galvanized products are preferred when the coated sheet is to be subjected to bi-axial deformation before its end use. Addition of silicon inhibits the formation of brittle intermetallic layer which reduces ductility and formability of final product. But occasionally addition of silicon is not sufficiently effective [22].

As for coating microstructure of the Galvalume<sup>®</sup> coating, two main phases are observed, one of which is aluminum rich dendritic phase, which begins with the solidification and the other one is inter-dendritic zinc rich phase. Figure 2.5 demonstrates the cross-sectional SEM image of a Galvalume<sup>®</sup> coating. Note that silicon existence is also observed [21].

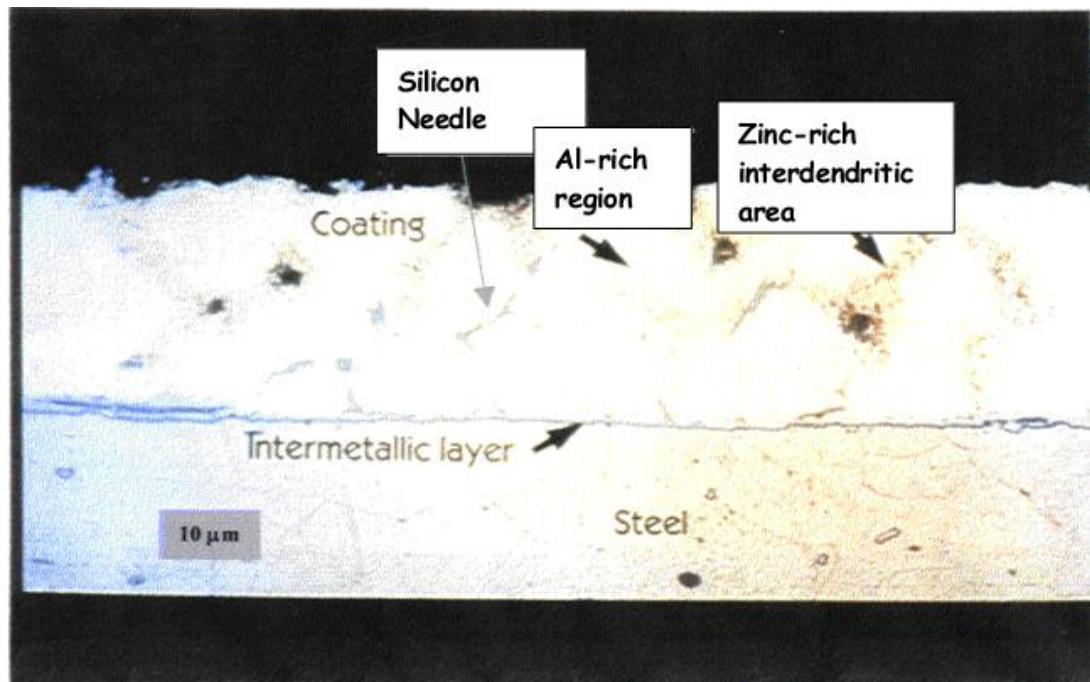


**Figure 2.5** SEM image of Galvalume<sup>®</sup> coating taken from the cross-section of a steel sample [21].

Owing to the high aluminum content, Galvalume<sup>®</sup> coatings also endure high temperatures. For instance they show no change of color up to 400 °C and no scaling up to 600 °C. Based on various in-situ experiments, Galvalume<sup>®</sup> coating has serviced dramatically longer than galvanized coatings and they find wide usage in various industries mainly building industry [21].

#### **2.3.4. Galfan<sup>®</sup>**

Galfan<sup>®</sup> is a coating type which has a coating bath consisting of 5 % Al and approximately 95 % zinc with additions of rare earths such as Ce and La in a range of 0.01 to 0.2 %. Rare earth additions aim better wetting of steel by molten metal bath and obtaining uniform thickness along the surface [26]. Some sources suggest rare earth element additions up to 0.5 % [27].

Galfan<sup>®</sup> is a registered trademark of Galfan Technology Center Inc. (GTC) first patented in 1981. It is widely licensed to various companies across the world. Additionally, ASTM A875/A875M and EN 10214 Standards are used for specifying Zn – 5 % Al coated sheet.

One main objective of the Galfan<sup>®</sup> processing is to obtain an intermetallic free zinc coating but many investigators suggest the formation of  $\text{Fe}_2\text{-Al}_5\text{-Zn}_x$  compound even after the short dipping times [25, 28]. The main corrosion protection principle of the Galfan<sup>®</sup> coating relies on the eutectic composition of zinc and aluminum at 5 % Al. In galvanizing, coating alloys solidifies as single-phase structured patterns while Galvalume<sup>®</sup> coating alloys solidifies as two phase microstructures. On the contrary, in Galfan<sup>®</sup> coating, a hypoeutectic microstructure in which high zinc containing and high aluminum containing phases solidify into very thin alternating parallel plates named lamellae, as can be seen on figure 2.6. Cooling rate control is vital to obtain lamellar structure [27].

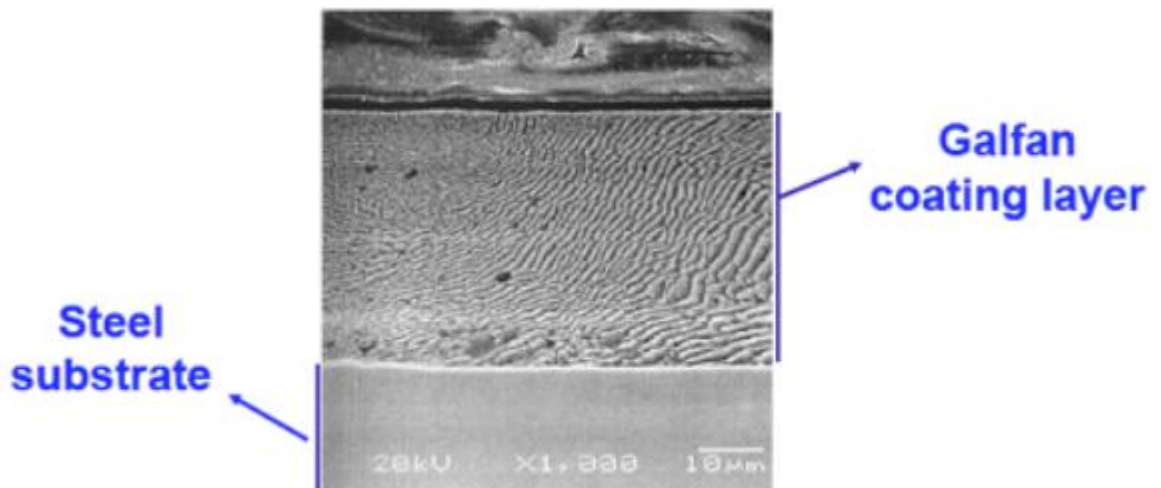


**Figure 2.6** Microstructure of Galfan<sup>®</sup> coating showing lamellar structure [27].

The intermetallic layer seen on the microstructure of the Galfan<sup>®</sup> coating is thinner than that of a regular galvanized coating and so it has an excellent formability. Table 2.6 provides some properties of the Galfan<sup>®</sup> relative to other types of coatings.

**Table 2.6** Comparison of Galfan<sup>®</sup> with other types of coatings [27].

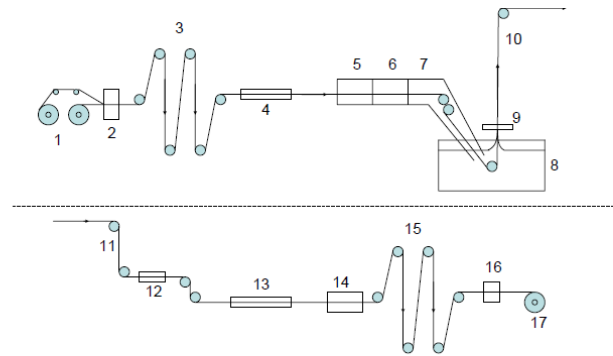
	<b>Galfan</b>	<b>Hot-Dipped Galvanized</b>	<b>Electro-Galvanized</b>	<b>Galvanneal</b>	<b>Galvalume</b>
<b>Formability</b>	5	3	5	3	3
<b>Corrosion Resistance</b>	4	3	3	2	5
<b>Sacrificial Protection</b>	5	5	5	5	3
<b>Corrosion Resistance (formed)</b>	5	3	3	3	3
<b>Paint Adhesion</b>	5	4	5	5	4
<b>Corrosion resistance (painted)</b>	5	4	4	5	3
<b>Weldability</b>	4	4	5	5	2
<b>Heat Resistance</b>	3	3	3	2	4

Note: 5 – Best ; 1– Worst

### 2.3.5. Galvanizing Line Hardware

Continuous galvanizing lines consist of many equipment and/or devices. This equipment is subjected to a very aggressive environment having elevated

temperatures and corrosive molten metals. Especially the pot hardware, guiding steel strip through molten metal bath, is critical for a continuous galvanizing line [6]. Figure 2.7 schematically summarizes a typical continuous galvanizing line [29].



- |                                      |                            |
|--------------------------------------|----------------------------|
| 1. Payoff Reels                      | 9. Air/Gas Knives          |
| 2. Seam Welder                       | 10. Up leg Cooling         |
| 3. Accumulator loop car 1            | 11. Down leg Cooling       |
| 4. Degreaser                         | 12. Galvanneal Furnace     |
| 5. Non Oxidizing Furnace (Annealing) | 13. Online Inspection      |
| 6. Radiant Tube Section              | 14. Chemical Treatment     |
| 7. Jet Cooling Section               | 15. Accumulator loop car 2 |
| 8. Molten Metal Pot (Zn/Zn Alloy)    | 16. Flying Shear           |
|                                      | 17. Carrousel Tension Reel |

**Figure 2.7** Overall picture of a continuous galvanizing line [29].

On continuous galvanizing lines, steel strip to be galvanized is degreased, acid pickled and flux cleaned before it enters into molten metal pot. With the help of one sink roll and two stabilizer rolls, it passes through galvanizing bath and excess zinc on surface of the steel strip is wiped off with air knives and goes to the cooling units. Following this procedure steel strip is inspected and winded into coils.

### 2.3.6. Sink Rolls

Sink rolls are used to pass the steel strip to be coated through the galvanizing bath on continuous galvanizing lines. It works in a very aggressive medium which is

corrosive at elevated temperatures. Schematic view of the galvanizing bath and sink rolls can be seen on figure 2.8.

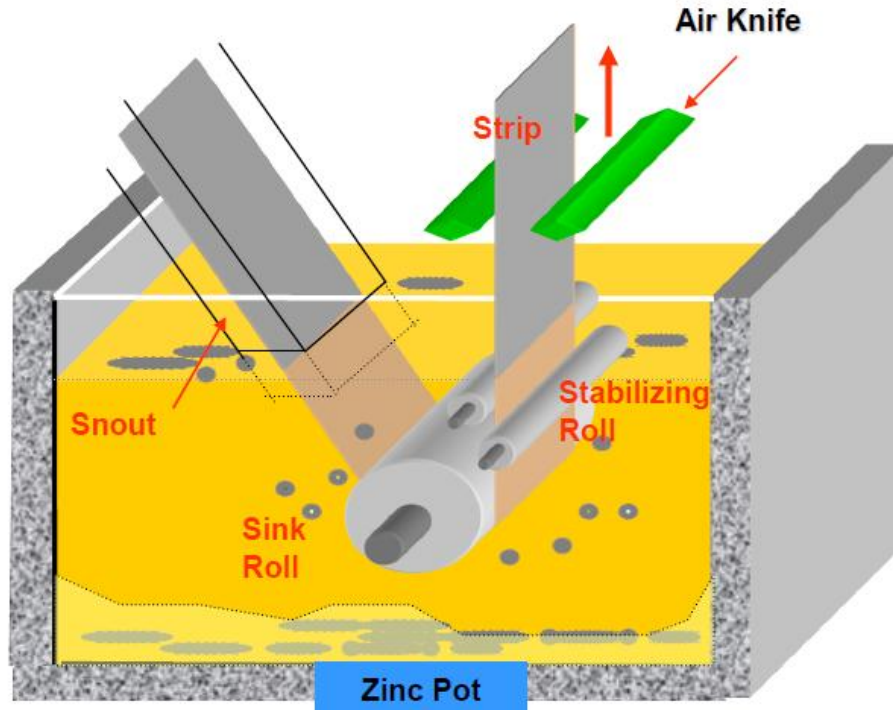


**Figure 2.8** Schematic view of galvanizing bath showing function of galvanizing hardware.

Bath hardware including sink roll, stabilizing rolls, and their bearings and bushings are the most critical equipment among all of the components of a galvanizing line for the reason that they need periodic maintenance and so they cause inevitable stoppage of the line. Stoppage due to the corrosion damage caused by liquid zinc and its alloys, to the bath hardware mean additional loss of time and cost. Therefore material selection for these rolls must be carried out carefully in order to minimize the problems mentioned above. AISI 316L stainless steel is the most common material grade for sink rolls since it has an optimum combination of corrosion resistance, mechanical properties and costs. In fact, various studies have been done in order to compare the possible galvanizing bath materials and AISI 316L steel have outperformed the most common martensitic and ferritic stainless steel grades while

exhibiting weak corrosion performance than some other metals, alloys or coated alloys [5, 30, 31].

## **2.4. Galvanizing Metallurgy with Bath Hardware**

It is an extensively known fact that most of the metals are extremely corroded by liquid zinc or zinc-aluminum alloys when they are exposed to such media. Therefore the hardware, servicing in the galvanizing bath, needs frequent maintenance and also needs to be replaced when its wall thickness is decreased to a level at which the roll falls behind the design requirements in terms of mechanical properties. Nevertheless sink rolls are servicing in the galvanizing baths for certain periods varying from 1 week to 3 weeks without maintenance. In this set of materials, an optimization could be done regarding minimum dissolution rate of the steel in zinc bath depending on the aluminum composition [2].

### **2.4.1. Effect of Aluminum**

During the continuous galvanizing operation, chemical interaction between steel and molten metal is explained in section 2.3 when there is no aluminum in galvanizing bath. Various phases, forming on the steel surface in absence of aluminum in the coating bath, show poor ductility and this renders them to have poor resistance to shear cracks and peeling during forming. This property of coating restrains the formability of the sheets into complex shapes such as drawn components or automotive fenders. When aluminum is introduced to the coating bath in a range of 0.14 to 0.19 wt. %, it inhibits reaction of zinc and iron ( $\text{FeZn}_7$ ) since it has a greater affinity to iron than zinc. Consequently, an aluminum-iron-zinc phase ( $\text{Fe}_2\text{Al}_{5-x}\text{Zn}_x$ ) forms on the surface of the steel. This thin, ternary phase usually consists of 45 % Al, 35 % Fe and 20-35 % Zn depending on the diffusion of the zinc into the  $\text{Fe}_2\text{Al}_5$  compound after the first contact of the steel with galvanizing bath. The aluminum-iron-zinc alloy reduces the diffusion rate of the zinc and affects the coating thickness

since it acts like a barrier to the reaction of iron and zinc as shown in figure 2.9 [32, 33].

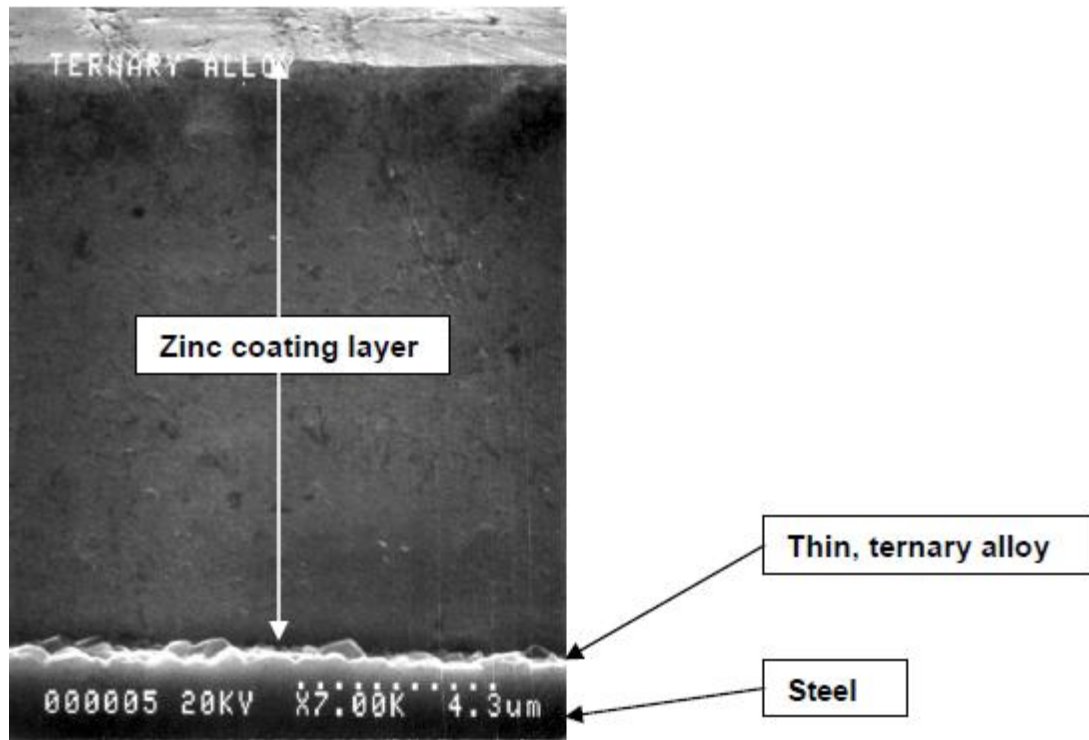


**Figure 2.9** Cross sectioned image of a galvanizing bath containing aluminum showing ternary Fe-Al-Zn alloy [32].

The aluminum content in the galvanizing bath also affects the corrosion rate of the sink rolls extremely. Pure zinc in molten state corrodes the surface of the sink rolls or other galvanizing bath hardware greater than the molten zinc-aluminum alloy because of the inhibiting characteristics of the ternary alloy of Fe-Al-Zn. In figure 2.10, the effect of aluminum concentration in the galvanizing bath can be clearly seen. Degradation rate of the AISI 316L stainless steel (most commonly used material grade for sink rolls and other bath hardware) in galvanizing bath decreases as the aluminum concentration of the bath increases. Even small variation of the aluminum level of the galvanizing bath affects the corrosion rate of the steel dramatically [32-34].

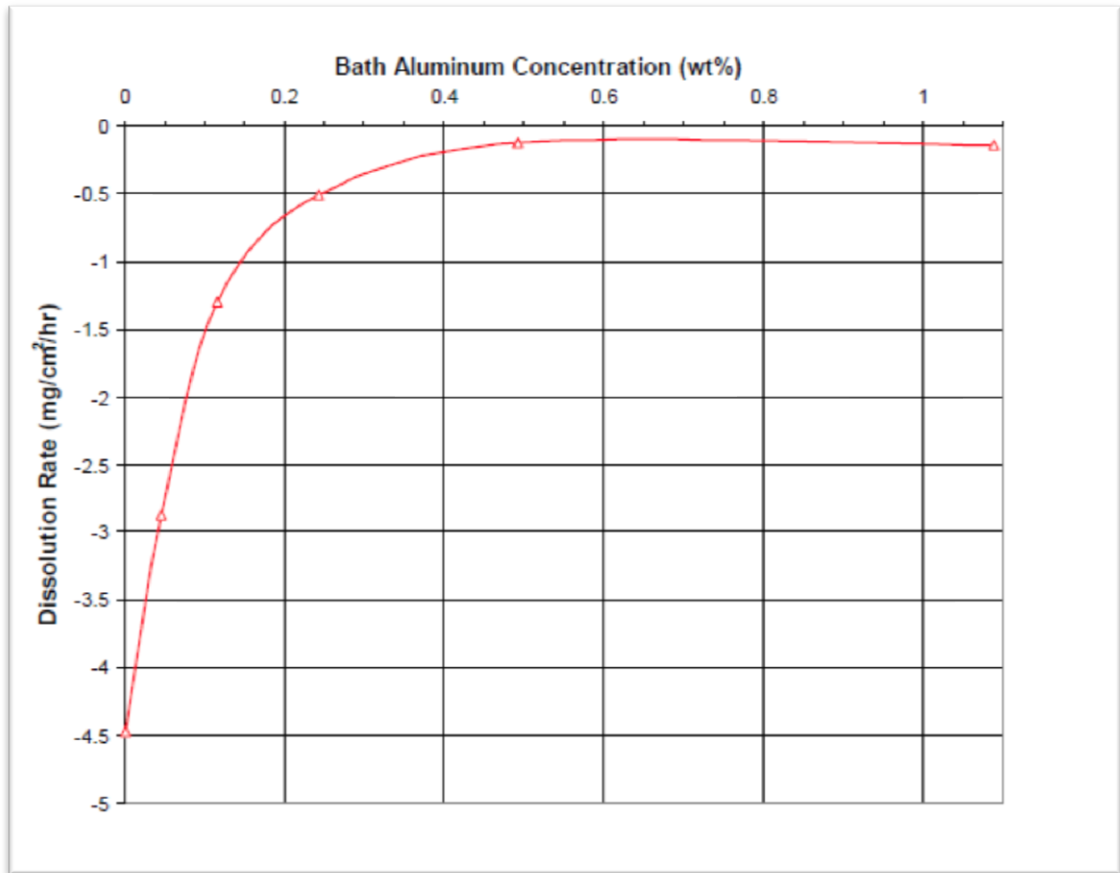


**Figure 2.10** Corrosion rate of the AISI 316L stainless steel depending on the Al concentration in galvanizing bath at 500 °C [2].

A sharp drop in the dissolution rate curve of the 316L steel around 0.14 wt % aluminum concentration can be observed from the figure 2.10. Along with these findings a phase transition from  $\delta$  to  $\eta$  phases is seen on the Zn-rich part of the Zn-Fe-Al phase diagram at 500 °C and 0.14 wt. % Al, figure 2.11. This phase transition is most widely known as “knee point”, at which galvanneal (GA) to Galvanize (GI) practices differ from each other in terms of chemical composition [34, 35].

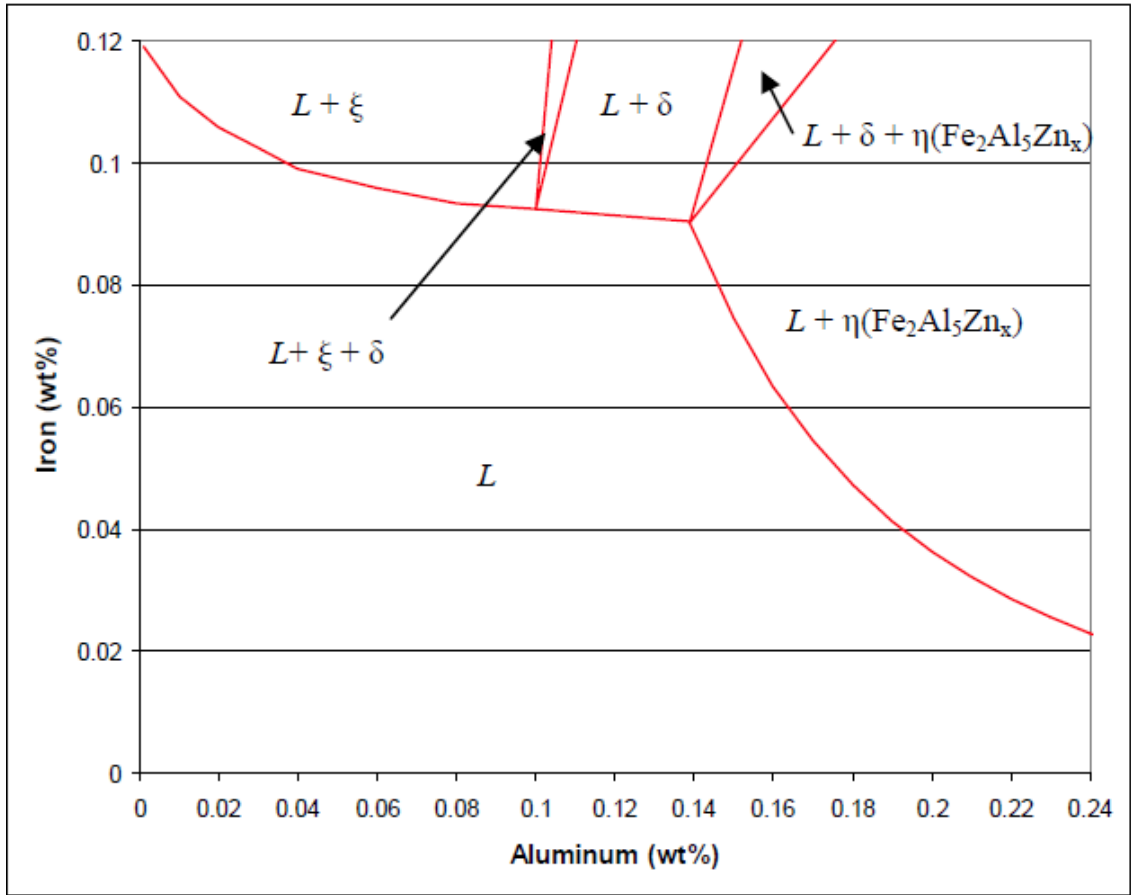


**Figure 2.11** Zinc-rich part of the Zn-Fe-Al phase diagram at 500 °C [35].

Aluminum content in the coating bath not only determines the coating type but also the corrosion characteristics of the coating bath towards bath hardware such as sink rolls and stabilizer rolls. Table 2.7 provides the aluminum contents for different types of coatings [18, 32, 34].

**Table 2.7** Aluminum contents of different types of coatings [18, 34].

Coating Type	Al Content range (wt. %)
Galvanize	0,14 – 0,20
Galvanneal	< 0,14
55% Al – Zinc	55
Galfan	5

#### **2.4.2. Role of Delta Ferrite in Austenitic Stainless Steels**

$\delta$  - Ferrite is a phase retained in most of the cast austenitic stainless steels during solidification. It has a body centered cubic crystal lattice and is discontinuously settled in the microstructure. Cast austenitic alloys have delta ferrite content in a range of 5 to 20 wt. % in general [10, 36].

Delta ferrite content in austenitic stainless steels brings some advantages as well as many disadvantages. It is present in some corrosion resistant cast austenitic stainless steels by design purposes. The reason of its presence is to increase weldability and corrosion resistance in specific corrosive environments. Fully austenitic stainless steels have poor weldability since they suffer welding problems such as hot cracking. This problem can be solved by using steel having approximately 4 % ferrite in its microstructure. For instance duplex CF grade stainless steels have immunity to weld cracking. Furthermore, certain concentration of ferrite in matrix improves stress corrosion cracking (SCC) resistance of some cast stainless steels. On the contrary, there are other studies stating that ferrite does not improve corrosion resistance regardless of the corrosive media or content. Preferential attacking to austenite or ferrite phases can be seen in different corrosive environments. Advantages of ferrite phase in terms of corrosion properties depend on the heat treatment history of the alloy and its service conditions [10].

As for the drawbacks of the delta ferrite phase in austenitic stainless steels, much can be said especially if the steel will be used at elevated temperatures. Metallurgical changes related to delta ferrite can introduce critical drawbacks at temperatures above 315 °C. When steels containing delta ferrite phase work at a temperature range of 425 to 650 °C, carbides preferentially precipitate at ferrite regions instead of austenite phase and this can lead to loss of mechanical properties if they are heated above 540 °C due to the formation of sigma or chi ( $\chi$ ) phases. At temperatures above 540 °C, these phases reduce toughness, corrosion resistance and creep ductility of the

steel. The reduction of mechanical properties can reach to extreme levels at which the V-notch Charpy energy of the steel at room temperature can be 95 % less than its original value [37, 38]. Moreover, deformation martensite can form from delta ferrite phase in low nickel containing stainless steels if cold working is applied. In case of acid chloride corrosion attack or electro-polishing of weld areas, delta ferrite phase dissolves preferentially instead of austenite [36]. In figure 2.12, optical microscope images of as weld condition of AISI 316L specimens having around 15 % delta ferrite can be seen [39].

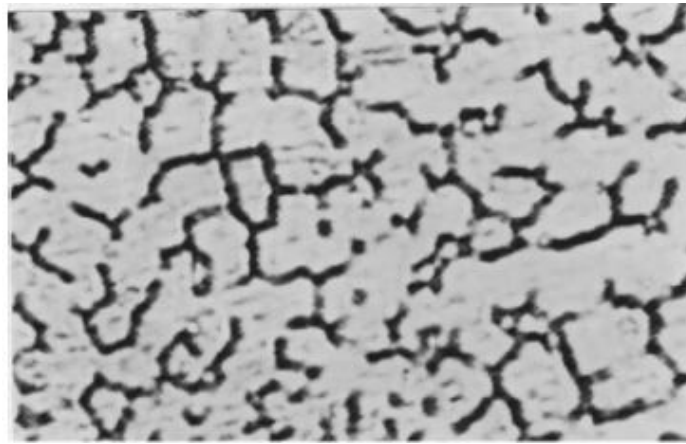


**Figure 2.12** Optical Microscope Image of 316L Stainless Steel showing delta ferrite phase (dark regions) [39].

#### **2.4.3. Control of Delta Ferrite in Austenitic Stainless Steels**

Delta ferrite content of the Austenitic Stainless Steels are extremely important since it affects field performance of these steels such as ductility, creep resistance, corrosion resistance, mechanical properties, weldability etc. Therefore, estimations of the delta ferrite contents of candidate austenitic stainless steels are vital before their actual utilization.

Some alloying elements promote the formation of delta ferrite in cast austenitic stainless steels while others inhibit. Various studies have been done and/or new technologies and devices have been introduced in order to estimate the delta ferrite content of stainless steels accurately. Naturally, none of them can make one 100 % sure about delta ferrite percentage of steel owing to the fact that an inevitable deviation occurs during detection of exact chemical composition of an alloy [10]. Following methods are the major ones used for predicting the delta ferrite phase percentage of the cast stainless steels.

#### **2.4.3.1. Schaeffler & Delong Diagrams**

Various efforts have been made using regression calculations of chromium and nickel equivalents directly influenced by austenite and ferrite promoting elements on the purpose of predicting the content of delta ferrite phase in stainless steels [40].

First of these calculations and constitution diagram generated by them belongs to Schaeffler and his diagram is represented in figure 2.13. The calculation method for predicting the delta ferrite content and phase distribution of the steel in subject is given in following equations 2.1 and 2.2 (all of the multipliers are considered as weight percent of the elements):

$$Cr_{eq}: Cr + Mo + 1,5 Si + 0,5 Nb \quad (2.1)$$

$$Ni_{eq}: Ni + 30 C + 30 N + 0,5Mn \quad (2.2)$$

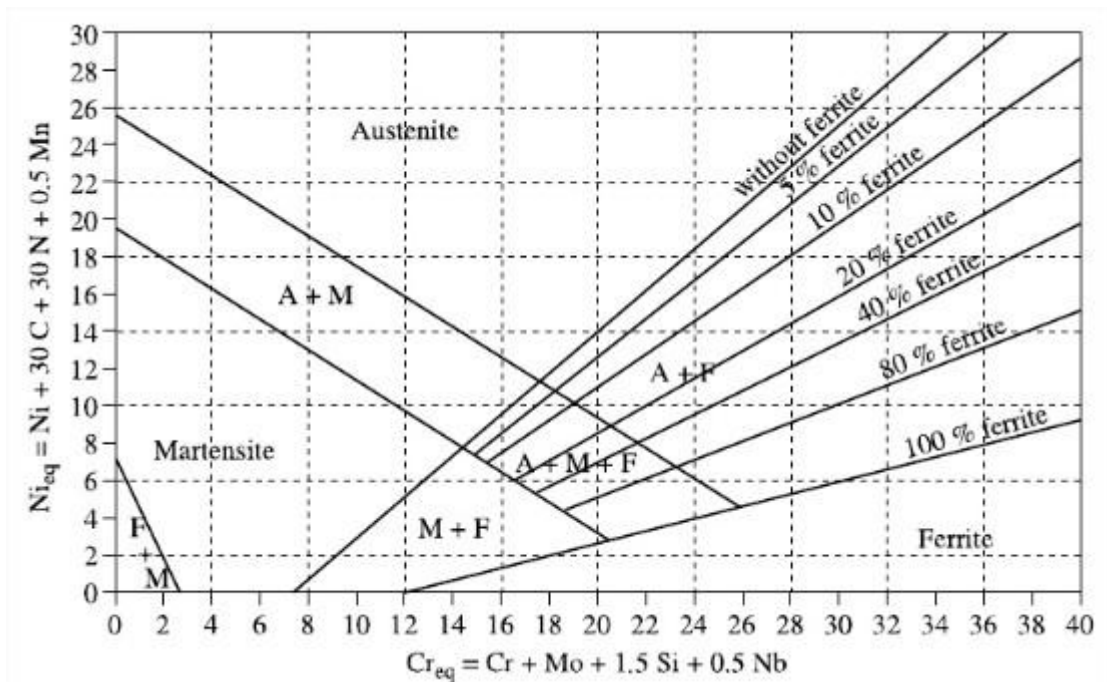


**Figure 2.13** Schaeffler's constitution diagram [41].

Schaeffler Diagram is one of the most accepted diagrams for predicting the delta ferrite in stainless steels and it still has a wide usage field in the industry. Schaeffler Diagram is asserted to provide a  $\pm 4$  vol. % ferrite precision for 78 % of cases [42].

Following Schaeffler's studies, DeLong revised Schaeffler's Diagram with taking nitrogen into account since it stands as a strong austenite promoter. DeLong's diagram can be seen in figure 2.14 and the equations for chromium and nickel equivalents are given in equation 2.3 and 2.4 [42].

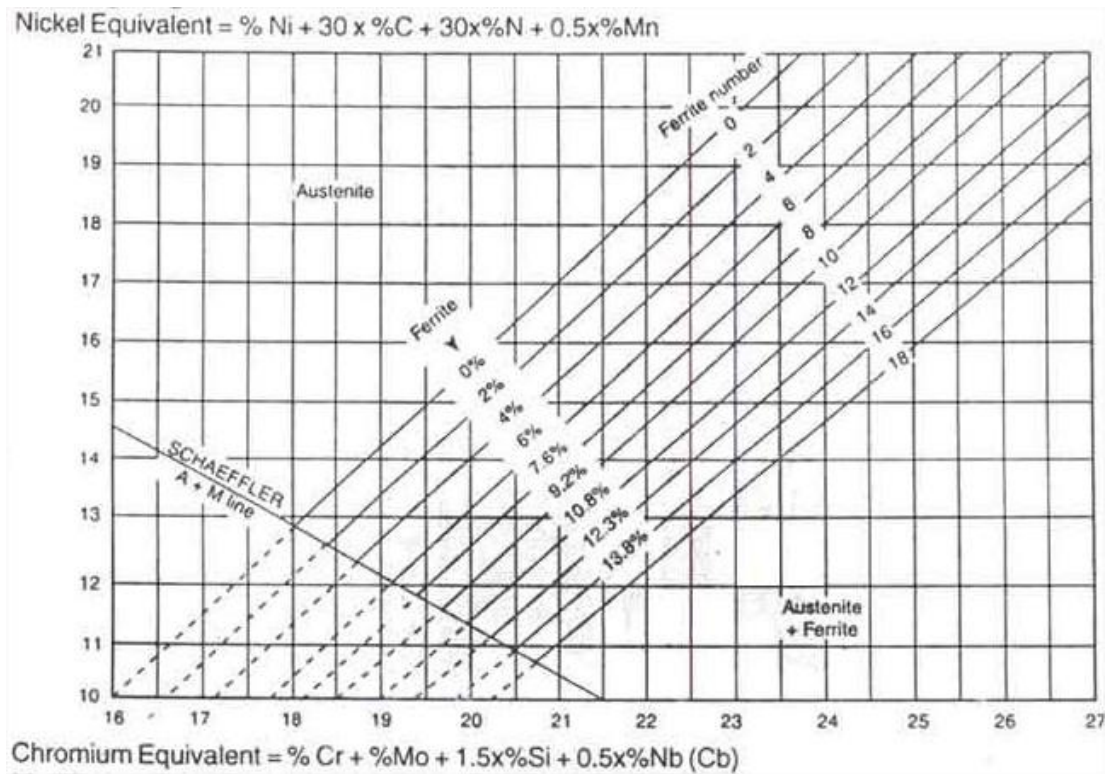


**Figure 2.14** DeLong's constitution diagram [43].

$$Cr_{eq}: Cr + Mo + 1,5 Si + 0,5 Nb \quad (2.3)$$

$$Ni_{eq}: Ni + 30 C + 30 N + 0,5Mn \quad (2.4)$$

### 2.4.3.2. Schoefer&WRC 1992 Diagrams

In 1974, Schoefer has developed his diagram for predicting the delta ferrite percentage in stainless steels. In his diagram, dashed lines shows the error interval of delta ferrite content represented in figure 2.15.

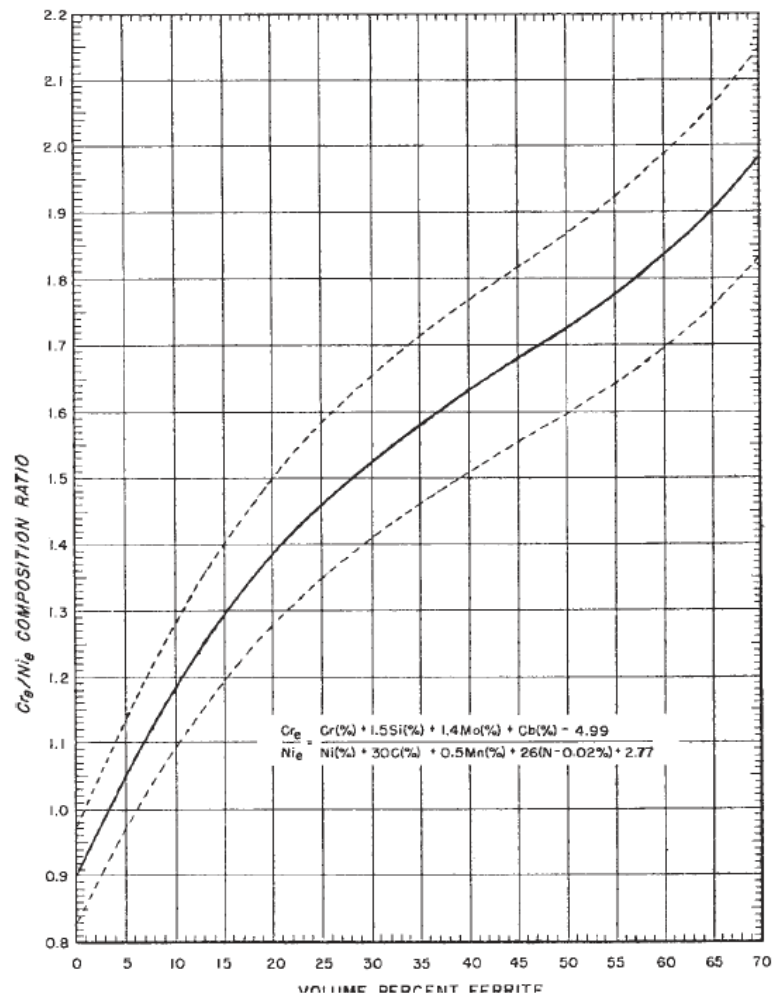


**Figure 2.15** Schoeffer's Diagram for predicting delta ferrite volume percent [44].

Unlike other delta ferrite predictor diagrams, in Schoeffer's diagram chromium and nickel equivalent ratio vs. volume percent ferrite is used. ASTM A800 [45] recognizes Schoeffer's diagram as its method for delta ferrite prediction. Equations 2.5 and 2.6 are the equations of the chromium and nickel equivalents of Schoeffer's diagram given as follows;

$$Cr_{eq} = Cr + 1,5 Si + 1,4 Mo + 0,5 Cb - 4,99 \quad (2.5)$$

$$Ni_{eq} = Ni + 30 C + 0,5Mn + 26(N-0,02) + 2,77 \quad (2.6)$$

In 1992, a new constitution diagram has been developed by Kotecki and Siewert which is given in figure 2.16 with the following calculations for chromium and nickel equivalents.

$$Cr_{eq}: Cr + Mo + 0,7Nb \quad (2.7)$$

$$Ni_{eq}: Ni + 35 C + 0,5Mn + 20 N + 0.25 Cu \quad (2.8)$$

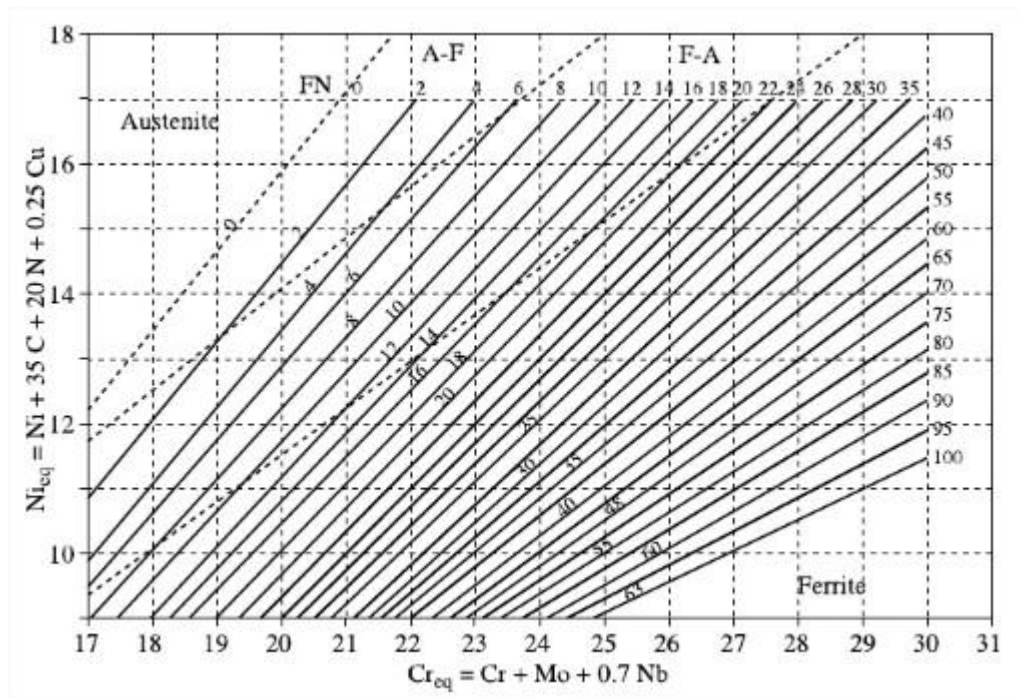


**Figure 2.16** WRC-1992 diagram [46].

WRC-1992 diagram has replaced DeLong's diagram in ASME III Code in 1994 and it still finds a wide usage field. However, it has major drawbacks because of the reduced number elements taken into account in calculating chromium and nickel equivalents. This problem limits its application fields [42, 47].

### 2.4.3.3. ORNL Diagram

ORNL (Oak Ridge National Laboratory) Diagram is a modified version of Schaeffler's Diagram for estimating ferrite content of stainless steels since they have reported that Schaeffler's diagram cannot be used for steels containing high manganese levels [48].

$$Cr_{eq}: Cr + 2 Si + 1.5 Mo + 5 V + 5.5 Al + 1.75 Nb + 1.5 Ti + 0.25 W \quad (2.10)$$

$$Ni_{eq}: Ni + Co + 0.5Mn + 0.3 Cu + 30 C + 25 N \quad (2.11)$$

Equations 2.10 and 2.11 are the formulas of modified version of Schaeffler's diagram by R. L. Klueh and P.J. Maziasz [48]. Using these formulas, a superimposed version of the Schaeffler's and ORNL's diagram is provided as can be seen in figure 2.17.

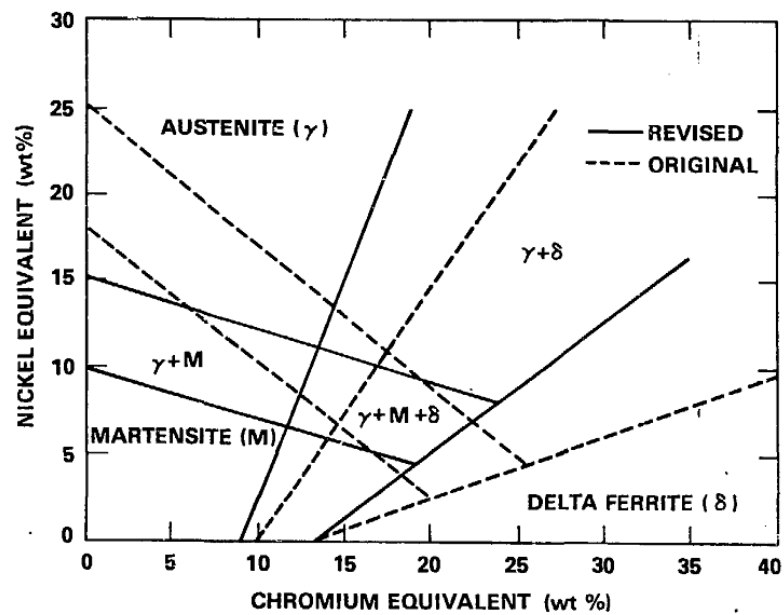


**Figure 2.17** Modified version of Schaeffler's Diagram by ORNL with original Schaeffler's diagram.

In figure 2.17, dashed lines represent the modification done by Klueh and Maziasz. Most attention grabbing part of this diagram is that the ferrite and austenite boundaries are shifted to the right according to their calculations. Because of the fact that they took many elements, which promote either ferrite or austenite, into account this diagram seems to be one of the most accurate one among major constitution diagrams [48].

#### **2.4.3.4. Feritscope<sup>®</sup>**

Feritscopes<sup>®</sup> are handheld devices using magnetic induction method to detect the delta ferrite, strain induced martensite or other non-magnetic phases such as sigma phase in stainless steels. They are extensively used in industry for ferrite measurement of the stainless steels. Testing of delta ferrite in stainless steels with a Feritscope<sup>®</sup> is a non-destructive method at which a magnetic interaction between two coils with the specimen is involved. First coil generates a magnetic field into the specimen and the changes in the magnetic field of the specimen due to the magnetic phases in it induce a voltage which is evaluated by the device [49, 50].

Feritscopes<sup>®</sup> are handheld and practical devices which allow users to determine instant ferrite content in stainless steel welds or materials. They have a user friendly interface and also the data in the devices can be transferred to computers as well. Furthermore User can easily perform measurement from curvy surfaces. As for the drawbacks of Feritscopes<sup>®</sup>, the result read on the device belong to all the magnetic phases in steel therefore it can include strain induced martensite or other magnetic phases as well as delta ferrite. If one seeks for specific delta ferrite content of a material, the exact delta ferrite content of the sample cannot be determined via Feritscope<sup>®</sup> since the magnetic phases are depending on the heat treatment, cold forming or other operations carried out on the material. Moreover, coated or dirty

surfaces strongly influence the results taken with these devices. International standards ISO 8249 and AWS A4.2 cover the usage of these devices [51, 52].

#### **2.4.3.5. Metallographic Methods**

Metallographic method for determining the delta ferrite content includes the point counting of the optically identified  $\delta$ -ferrite phase from the 2D image of the properly prepared sample. It has been extensively accepted that the volume % delta ferrite content of the steel is proportional to the area of the phase observed on the microscope image [42].

When adequately performed, using optical microscopy is a perfect way to determine the delta ferrite phase content of stainless steels. However, it has some drawbacks such as the influence of homogeneity, operator interpretation faults, effect of sample preparation quality, and deviation of the magnification of the image. These drawbacks cause the variation between the results taken from different laboratories [50].

This method is explained in detail in the ASTM standard E562 which also states that metallographic method is not only applicable to the delta ferrite phase detection in stainless steels but also applicable to any secondary phase properly identified by metallographic techniques [53].

### **2.5. Thermally Induced Embrittlement**

Microstructures of the stainless steels are easily affected during their services at elevated temperatures above 425 ° C. naturally; this renders them to be weaker than their original performance. Prolonged exposure to the elevated temperatures causes

austenitic stainless steels to become poor corrosion resistant, brittle mechanical behavior or both [54].

### **2.5.1. Sensitization**

Sensitization is the precipitation of the carbides (mainly as  $M_{23}C_6$  and  $M_7C_3$ ) at the grain boundaries of austenitic stainless steels which causes them to lose their toughness and corrosion resistance. “M” stands for “metal” at the  $M_{23}C_6$  and it is generally chromium due to its low diffusion rate at elevated temperatures relative to other elements present in austenitic stainless steels. Chromium and carbon are separated from each other at temperatures above 1035 °C but if the stainless steel is cooled slowly from 815 to 425 °C or reheated to this range, carbides mentioned above form and precipitate at the grain boundaries of the steel as schematically shown in figure 2.18. Consequently, the regions next to grain boundaries run out of chromium and lose their stainless features. This makes a way for intergranular corrosion in steel and these steels are said to be sensitized in literature. Loss of toughness is also observed in sensitized stainless steels. Welding the austenitic stainless steels is the most common cause of sensitization and it is also known as weld decay which can be seen in figure 2.19 [54, 55].

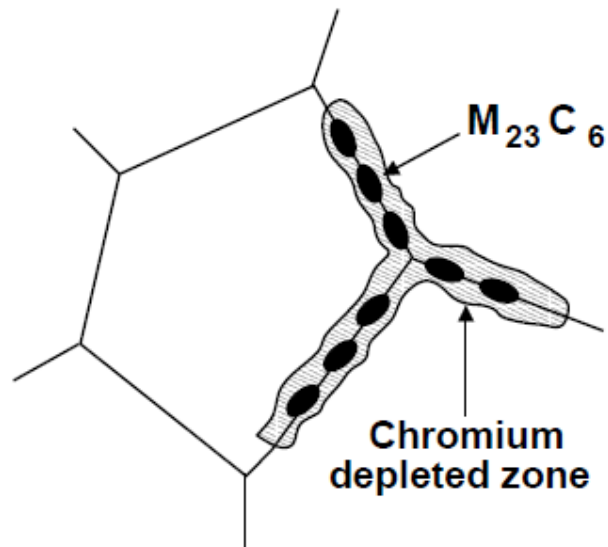


**Figure 2.18** Chromium depletion due to the carbide precipitation at the grain boundaries of steel [56].

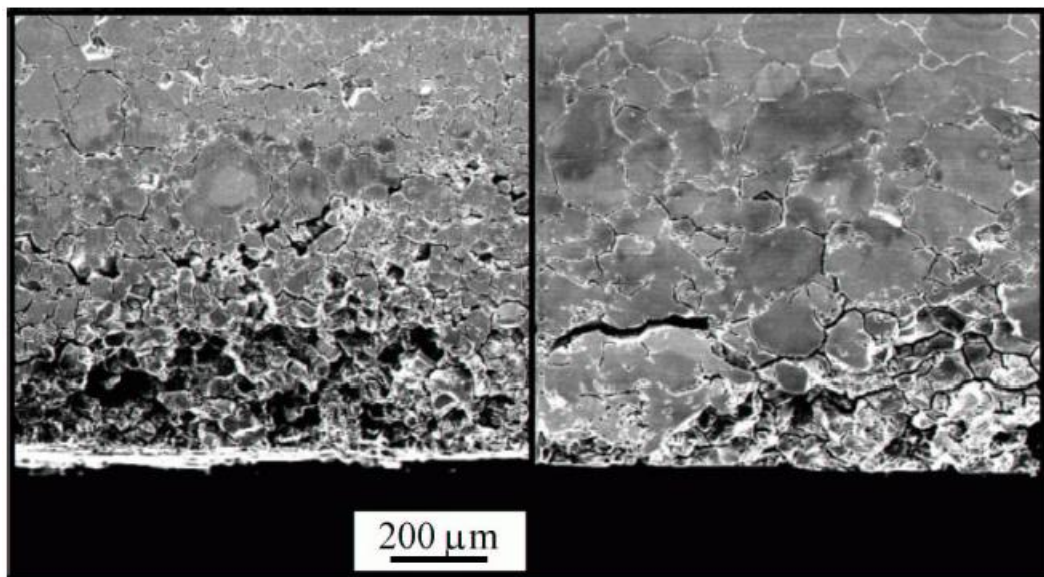


**Figure 2.19** Micrographs of the weld decay caused by intergranular corrosion of stainless steel [57].

Certain ways exist to avoid sensitization of the austenitic stainless steels during their high temperature services. The easiest one is to prolong the service – if possible – till the desensitization occurs. Holding the steel at the sensitization temperature results in

chromium diffusion to the chromium depleted zones and so the sensitization of the steel is reverted [58]. Second way to avoid sensitization is to reheat the material above 1035 °C and rapid cooling it so that the carbides are dissolved in matrix. Third way is to use “L” grades which have very low carbon content (0.03 max.) for high temperature applications but this method is not an exact solution since sensitization will also take place in low carbon grades. A better solution, fourth way, would be the use of stabilized austenitic grades such as AISI 321 and AISI 347 for the applications which will cause sensitization of common austenitic stainless steel grades. Stabilized grades contain titanium or niobium elements which combine with carbon before any other element in steel so they prevent the chromium carbide precipitation and sensitization. These grades have a stabilizing heat treatment at approximately 900 °C in order to take chromium to solution while combining titanium and niobium carbides [54].

### **2.5.2. 475 °C Embrittlement**

In case of prolonged exposure to a temperature range of 400 to 550 °C, stainless steels containing higher than 13 % chromium are susceptible to embrittlement called “475 °C Embrittlement”. This strongly affects the mechanical properties of them; increase in tensile strength and hardness while decrease in tensile ductility, impact energy and corrosion resistance are observed. Even though it is said that 475 °C embrittlement is seen in stainless steels having higher than 13 % chromium, this embrittlement mechanism is mainly experienced in ferritic and duplex grades but not in austenitic grades [10].

Multiple studies have been done in order to clarify the 475 °C embrittlement. Early theories were suggesting that precipitation of the second phases such as phosphides, carbides, nitrides or oxides were causing this embrittlement [59-63]. It turned out that these suggestions were not the explanation of this phenomena but a further study reported that a chromium rich bcc phase which have a lattice parameter slightly

greater than iron rich bcc ferritic matrix precipitates and this causes the embrittlement. These precipitates consist of approx. 80 % chromium and their sizes are in a range of 15 to 30 nm in diameter in a Fe-27Cr steel aged at 480 °C for 10000 to 34000 hours [64]. Further work on this subject has come to the conclusion that 475 °C embrittlement was a precipitation-hardening phenomenon resulting from the presence of a miscibility gap in the iron-chromium system below 600 °C. At the beginning of the 475 °C aging, between 20 to 120 hours, rate of hardening in steel increases exponentially due to the homogenous precipitation of the chromium-rich phase. Following this period of time, the rate of hardening continues but much slowly between 120 to 1000 hours and aging beyond 1000 hours causes only a little increase in hardness since the precipitates do not overage larger than approximately 30 nm [65].

The embrittlement level of the alloy depends on its chromium content; higher chromium content means higher degree of embrittlement. Carbide forming elements such as molybdenum, vanadium, niobium and titanium tend to increase the embrittlement as well as increased levels of carbon and nitrogen. Prior cold working also increases the embrittlement level of 475 °C embrittlement. 475 °C embrittlement can be reverted back even the alloy is extremely influenced. Heating it to 675 °C or higher temperatures for a small period of time will neutralize the detrimental effects of 475 °C embrittlement [63, 66].

### **2.5.3. Sigma Phase Embrittlement**

Sigma phase is a hard and brittle phase forms in ferritic, duplex or austenitic stainless steels. It renders them to have poor resistance against inter crystalline corrosion since it is not chemically resistant. It has a body centered tetragonal crystal lattice and it is usually seen in stainless steels having 18 % chromium or higher and 8 to 30 % nickel elements. Some alloying elements such as molybdenum, titanium, vanadium,

aluminum, niobium and especially silicon promote the sigma phase formation while higher contents of manganese and nickel suppress its formation [67].

Sigma phase results from long term exposure of austenitic, ferritic and duplex stainless steel to a temperature range of approximately 560 to 980 °C. Slow cooling of steel from 1040 to 1150 °C or reheating it to 560 to 980 °C cause sigma phase precipitation. Formation of sigma phase extremely reduces impact strength of stainless steels containing ferrite. The strongest effect of sigma phase to the impact strength of the steel is observed when the steel is cooled below 260 °C. The steel exhibits 100 % brittle behavior when it is cooled below 260 °C while it can conserve its toughness above that temperature [54, 67].

In the design stage of the stainless steels which will service at elevated temperatures, it would be advantageous to know if sigma phase will be formed during its service. The susceptibility of sigma phase formation can be estimated via following formula proposed by Hull in 1973 [68]:

$$\text{ECC} = \text{Cr \%} + 0,31\text{Mn \%} + 1,76\text{Mo \%} + 0,97\text{W \%} + 2,02\text{V \%} + 1,58\text{Si \%} + 2,44\text{Ti \%} + 1,70\text{Cb \%} + 1,22\text{Ta \%} - 0,266\text{Ni \%} - 0,177\text{Co \%} \quad (2.12)$$

Where “ECC” stands for “Equivalent Chromium Content”.

If the equivalent chromium content is greater than 17- 18 %, the stainless steel in subject tends to suffer from sigma phase formation. The effect of sigma phase to the corrosion behavior of the stainless steels is strongly similar to the sensitization since both of chromium carbides and sigma phase form at similar temperature ranges. Stainless steel with sigma phase can suffer from intergranular corrosion as it is in

case of the sensitization. Even though formation of sigma phase is generally related with the  $\delta$ -ferrite, it can also form directly from austenite matrix [54, 67].

## CHAPTER 3

### EXPERIMENTAL PROCEDURE

#### 3.1. Sample Production of Candidate Steels

As previously mentioned in chapter 1, 5 candidate steels, all of which are containing carbon equal or less than 0.03 weight percent are tested in this study. 4 of these candidate steels are new developed alloys for this study while one of them is AISI 316L which is the most common stainless steels used as galvanizing line sink roll material. All of them are centrifugal cast by a foundry in Sweden with the chemical compositions represented in table 3.1.

**Table 3.1 Chemical Compositions of five candidate steels tested in this study**

Steel No	C	Si	Mn	P	S	Cr	Ni	Mo	Others
1	0.018	0.330	10.180	0.020	0.004	23.700	8.500	2.230	N,Cu,V,W
2	0.003	0.409	1.040	0.005	0.006	24.040	11.160	2.060	N,Cu,V,W
3	0.004	0.443	8.070	0.006	0.005	18.950	9.240	2.500	N,Cu,V,W
4									
(AISI 316L)	0.016	1.050	0.970	0.015	0.013	19.970	9.320	2.260	N: 0.123
5	0.024	0.320	1.730	0.010	0.005	24.070	13.360	2.060	N,Cu,V,W

Candidate steels are supplied in form of tubes having outer diameter of 400 mm, inner diameter of 311 mm and length of 370 mm. They are solution annealed at 1100 °C for three hours after casting in order to solve all carbides and nitrides in their microstructure. Subsequently they are water quenched and their outer surfaces are rough machined as can be seen in figure 3.1.



**Figure 3.1** Candidate steels in form of tubes.

### **3.2. Delta Ferrite Determination**

Delta ferrite contents of the steels are determined and recorded before further testing. As previously explained in 2.5.3, one method would not be sufficient to be sure about the delta ferrite content of stainless steels. For this reason, delta ferrite

measurements are carried out such a way that different methods have confirmed each other.

Firstly, metallographic method is used for determination of the delta ferrite contents of candidate steels. Samples have been extracted from steel tubes, have been ground on automated wet sanding device and polished with 6, 3, 0.3 $\mu$  polishers respectively. Etching is done with 100 mL HCl + 25 g. picric acid solution in order to reveal austenite/ferrite boundaries explicitly. Subsequent to these operations, metallographic specimens are 2D imaged via Olympus PMEU – F200 Optical Microscope and delta ferrite content is determined using QCapture Pro V. 5.1.1.14 Software.

As a second method, an AWS Calibrated Feritscope® FMP 30, this is seen in figure 3.2, produced by Company Helmut Fischer GmbH, Germany. Feritscope® is calibrated with its calibration blocks which made it capable of measuring delta ferrite phase in a range of 0 to 100 %. Then delta ferrite contents of the steel samples have been determined and recorded.



**Figure 3.2** Feritscope® FMP30.

Along with these two methods, estimations of the delta ferrite contents of the candidate steels are also done using Schaeffler's, Delong's, Schoeffer's, WRC-1992 and the modified version of Schaeffler by Oak Ridge National Laboratory (ORNL) Diagrams in an effort to be sure about the delta ferrite contents.

### **3.3. Corrosion Testing**

In this study, immersion corrosion tests which involve the simulation of the galvanizing bath (molten zinc-aluminum alloy) have been carried out. Steel specimens belong to candidate steels have been immersed into the miniature galvanizing bath. Some of them are taken out from the bath at different time intervals. After removal, their coatings are acid pickled and their weight losses due to the molten metal corrosion are measured as detailed in next subtopics.

#### **3.3.1. Corrosion Specimen Preparation**

Twenty corrosion specimens which have been used in corrosion tests are cut from the steel tubes and precise machined to the below dimensions. One bore drilled on each of them in order to hang them down to the galvanizing bath.

Diameter: 40 mm

Length: 4 mm

Surface Area: 3025 mm<sup>2</sup>



**Figure 3.3** Immersion Corrosion Test Specimens.

All twenty specimens are carefully marked and one set (5 specimens) of them are age treated at 750 °C for comparison after the test. Thereafter weights of them are recorded with analytical balance Radwag AS 220/C/2 which has a sensitivity of 0.1 mg. Finally they were ready after cleaning with alcohol. All preparation steps of the corrosion samples were in accordance with ASTM G 01 – 03; Standard Practice for Preparing, Cleaning, and Evaluating Corrosion Test Specimens [69].

### **3.3.2. Immersion Corrosion Tests**

In this set of experiments, laboratory scale immersion corrosion tests have been carried out in accordance with ASTM G31 – 72 (reapproved 2004); Standard Practice for Laboratory Immersion Corrosion Testing of Metals [70].

A miniature galvanizing bath is produced in order to simulate the galvanizing media and immerse the specimens in it. It is an electric resistance heated furnace with a power of 380 kW with a 10 liter SiC/Graphite crucible. Temperature control system of the furnace is important to maintain the temperature precisely since the temperature differences causes major problems. Therefore the temperature control system of the furnace is chosen as solid state relay (SSR) module which is capable of controlling the temperature in a range of  $\pm 1$  °C.



**Figure 3.4** Melting Furnace

In figure 3.4, actual photograph of the electric furnace which is used to simulate galvanizing media is seen before its usage. It has two thermocouples integrated to its SSR module, one of which is located between the electrical resistance and the crucible and the other one is immersed to the molten zinc aluminum alloy. Second thermocouple which is immersed to the molten metal has silicon carbide (SiC) cover in order to avoid the corrosive damage caused by molten zinc-aluminum alloy.

Before the immersion of the specimens prepared for immersion corrosion testing (see previous sect. 3.3.1), furnace is charged with pure (99.99 %) zinc ingots, each of them having approximately 7.5 kg. During the charging operation, it is critical to

leave space for expansion since ingots will be elongated due to the thermal expansion when they are heated to the melting point. Afterwards furnace is heated to the 200 ° C for 3 hours with the aim of evaporate the physical water in ceramic crucible and other volatile elements in zinc ingots. Then the temperature has risen to 550 ° C, which is notably higher than the melting point of the zinc, because of the latent heat to be given to the zinc ingots with the purpose of melting them. After the liquid zinc is obtained in the crucible, slag is taken from the surface of it and it is alloyed with pure aluminum wires to the levels at which the galvanizing media is attained. After this point, corrosion specimens are immersed into the molten zinc aluminum alloy with the help of hooked up pure titanium wires from their holes represented in figure 3.5. The titanium wires are replaced every 3 days for the reason that they are ruptured from their molten metal – air interfaces because of the corrosion. Periodically, chemical composition of the galvanizing bath is controlled with taking zinc samples from it. Additional aluminum and/or zinc are charged whenever it was necessary.



**Figure 3.5** Photograph of corrosion specimens to the molten zinc-aluminum alloy hooked up with wires.

4 sets of corrosion specimens are immersed into the bath. Each set consists of 5 specimens and 1 set of them are taken out from the galvanizing bath after 168h. Other 3 sets are taken

out from it after 504 hours. Table 3.2 summarizes the corrosion tests in terms of time intervals and heat treatment conditions.

**Table 3.2** Corrosion test conditions

<b>Steel Set</b>	<b>Heat Treatment Condition</b>	<b>Exposure Time (hour)</b>
<b>A</b>	Aged at 750 ° C	504
<b>B</b>	Solution Annealed	168
<b>C</b>	Solution Annealed	504
<b>D</b>	Solution Annealed	504

Each set of corrosion specimens written on table 3.2 consist of 5 specimens of different steel types. Set A has a different heat treatment condition while set B has a shorter exposure time than other series. All of the corrosion specimens taken out from galvanizing bath have been preserved in non-oxidizing environments until their coatings have been removed. Visual evaluations have been done with their coated conditions.

### **3.3.3. Pickling of Coatings**

Immersion corrosion test specimens taken out from the bath are acid pickled according to the standard ASTM G 01 – 03; Standard Practice for Preparing, Cleaning, and Evaluating Corrosion Test Specimens [69]. The acidic solution used to remove the galvanize coating was dilute hydrochloric acid (HCl) produced by Sigma Aldrich which has 37 % concentration. The HCl solution is diluted to the 15 % concentration with distilled water and placed to the ultrasonic cleaner in a glass beaker. Pickling operation is carried out in fume hood with necessary precautions such as protective gloves, masks and filters.

### 3.3.4. Corrosion Damage Evaluation

Pickled and cleaned corrosion specimens are weighed with the analytical balance Radwag AS 220/C/2 which has a sensitivity of 0,1mg. Then the values are subtracted from the initial weights of the corrosion specimens therefore the weight loss of the specimens due to the molten metal corrosion is obtained. In cleaning of the specimens for weight loss determination, standard ASTM G 01 – 03; Standard Practice for Preparing, Cleaning, and Evaluating Corrosion Test Specimens[69] is used. In this operation, it is vital to pickle the specimens properly because excess corrosion caused by HCl during the pickling dramatically affects the weight loss results. For this reason, the cleaning procedure is repeated several times and specimens weighed after each cleaning procedure. During repeated cleaning operations, mass loss of the specimens are recorded and visually controlled in order to be sure about the complete removal of the coatings with not removing excess metal from specimens. Finally, corrosion rates of the specimens are determined with the following equation described in ASTM G 01 – 03:

$$\text{Corrosion Rate} = (K \times W) / (A \times T \times D) \quad (3.1)$$

Where:

K= a constant, which is chosen as grams per square centimeter per hour ( $\text{g} / \text{cm}^2 \text{ h}$ ) =  $1 \times D$  (density)

T= time of exposure in hours

A= surface area in  $\text{cm}^2$

W= mass loss in grams

D= density in  $\text{gr.} / \text{cm}^3$

### 3.4. Mechanical Tests

Mechanical Tests have been conducted to the specimens extracted from candidate steel rings. Charpy impact tests and tensile tests are conducted to the specimens at 4 different heat treatment conditions explained as follows.

#### 3.4.1. Sample Preparation and Heat Treatment

40 Tensile test specimens and 60 impact test specimens were extracted from 5 steel rings which have candidate chemical compositions. It is designed to have 2 specimens for each tensile test and 3 specimens for impact tests. Photograph of the mechanical testing specimens can be seen on figure 3.6.



**Figure 3.6** Photo of mechanical test specimens as cut from rings.

Firstly, mechanical testing specimens are cut from the steel rings with machining allowances. Then they are rough machined to the dimensions approximately 5mm higher than their final dimensions. Following rough machining, specimens are heat treated to the conditions written on table 3.3. It is important that specimens shall be

wet-cut since stainless steels can easily strain hardened which would affect the mechanical testing results dramatically.

**Table 3.3** Heat treatment conditions and time intervals.

<b>Condition</b>	<b>Period</b>
<b>Solution Annealed</b>	3 hours then water quenched
<b>Galvanizing Temp (460 ° C)</b>	504 hours
<b>Age Treated (750 ° C)</b>	16 hours then water quenched
<b>Age Treated + Galvanize Temp</b>	16 hours water quenched then 504 hours at 460 ° C

4 different heat treatment conditions with 5 different steels ended up in 20 tensile tests each consist of 2 specimens which make 40 in total. Similarly, 20 Impact tests each consist of 3 specimens required 60 specimens in total. These specimens are heat treated in a small annealing furnace Protherm PLF 120/10, having max working temperature of 1210 ° C and internal volume of 10 liters.

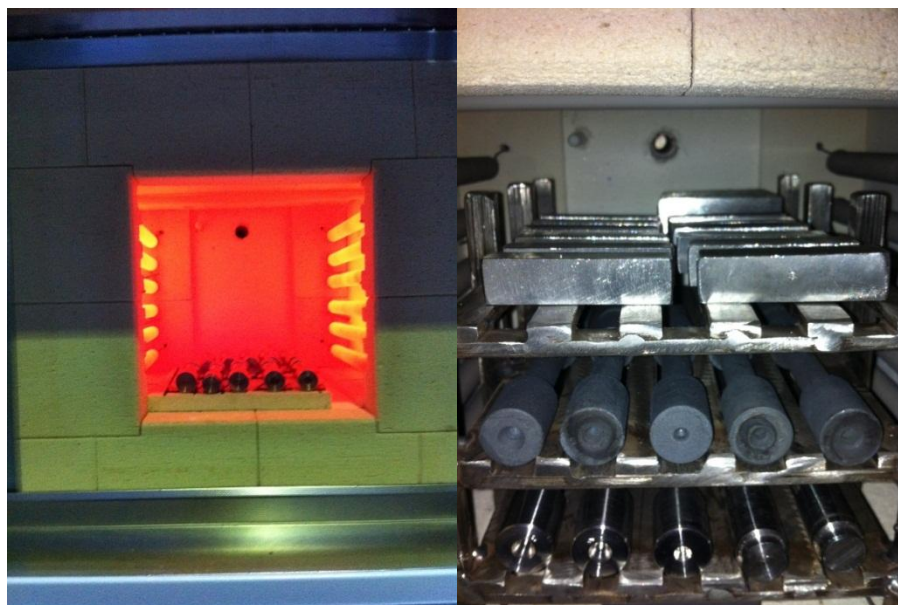


**Figure 3.7** Heat treatment of rough machined mechanical test specimens in annealing furnace.

Following heat treatment, the specimens were precisely machined to their final dimensions and cleaned in ultrasonic cleaning device. Visual controls have been done in order to avoid notch, crack or surface defects on them. Finally, all of them are prepared for actual testing.

### 3.4.2. Tensile & Charpy Impact Tests

In tensile testing of this study, Tensile Testing Device Instron 5582 having a 100 kN of load capacity is used. Tensile testing is conducted in accordance with the standard EN 10002 – 1; Metallic Materials – Tensile Testing – [71].

Pendulum type Tinius Olsen Impact Testing Machine is used to carry out the impact tests. They are conducted according to the standard ISO 148-1:2009 Metallic materials – Charpy pendulum impact test – Part 1: Test method [72]. Figures 3.8 and 3.9 represent the tensile testing machine and impact testing machine respectively.



**Figure 3.8** Tensile testing device



**Figure 3.9** Impact Testing Machine

### **3.5. Scanning Electron Microscopy (SEM) Characterization of Galvanizing Bath**

For the purpose of being sure that the galvanizing media is achieved in simulating the galvanizing bath, scanning electron microscopy techniques are used for characterization of the coating. In order to characterize the microstructure & chemical composition of the coatings, JEOL JSM-6400 Electron Microscope is used with its energy dispersive spectroscopy (EDS) unit integrated on it. A photograph of the SEM is given in figure 3.10.



**Figure 3.10** SEM used for microstructural characterization

## **CHAPTER 4**

### **RESULTS AND DISCUSSION**

In this study, 4 new stainless steel compositions are developed and tested in order to enhance the corrosion and mechanical performance of the sink rolls used in continuous galvanizing lines. Currently, AISI 316L is most widely used in fabrication of sink rolls. Thus, AISI 316L is also tested with 4 new stainless steel alloys in order to compare the results. As it is mentioned on sections 2.3.2 and 2.3.3, delta ferrite content in stainless steels affects their corrosion performance significantly. So that the delta ferrite contents of the 5 stainless steels, tested in this study, have been determined with 3 different methods in order to be sure about their exact delta ferrite content.

Following delta ferrite determination, immersion corrosion tests have been carried out to the samples of 5 different candidate steels in a simulated galvanizing medium. In order to be sure that exact galvanizing media is attained in molten zinc – aluminum bath used in the corrosion testing of this study, coating morphology and chemical composition are examined via SEM-EDS techniques. Intermetallic phases and their chemical compositions detected during SEM-EDS studies have matched to the ones found in literature. These results confirmed that galvanizing medium used in this study is very close to typical industrial baths. Consequently, corrosion performances of 5 stainless steels have been compared with each other in terms of mass losses and corrosion rates.

Finally, mechanical testing of 5 candidate steels has been carried out after subjecting them to different heat treatment regimes. Solution annealed, conditioned to galvanizing heat regime (460 °C for 21 days), age treated (750 °C for 16 hours) and both conditioned to galvanizing heat regime and age treated mechanical testing results are obtained and compared with each other. Consequently, their mechanical behaviors are discussed.

#### 4.1. Delta Ferrite Determination

Firstly, estimation of the delta ferrite contents of 5 candidate steels is carried out using ORNL Diagram since it gives almost same results with the metallographic image analysis method and feritscope® measurements [48]. Table 4.1 represents the delta ferrite contents of 5 candidate steels measured with feritscope®. As a confirmation of feritscope® measurements, metallographic image analysis method is used for steel 5 which can be seen on figure 4.1.

**Table 4.1** Delta Ferrite Measurement Results with Feritscope®.

<b>Steel</b>	<b>Delta Ferrite (%)</b>
<b>1</b>	2.93
<b>2</b>	3.06
<b>3</b>	2.49
<b>4 (AISI 316L)</b>	5.61
<b>5</b>	2.50

As can be seen on table 4, candidate steels have different delta ferrite contents depending on their chemical compositions. Some of them have more austenite promoting elements such as Ni, Mn, N while others have more ferrite promoting elements such as Cr, Mo, V, Cu etc. It is vital to obtain exact values since delta

ferrite contents strongly affect the corrosion performance and mechanical properties of these alloys. For these reasons, more than 1 method is used for delta ferrite determinations [36, 37].

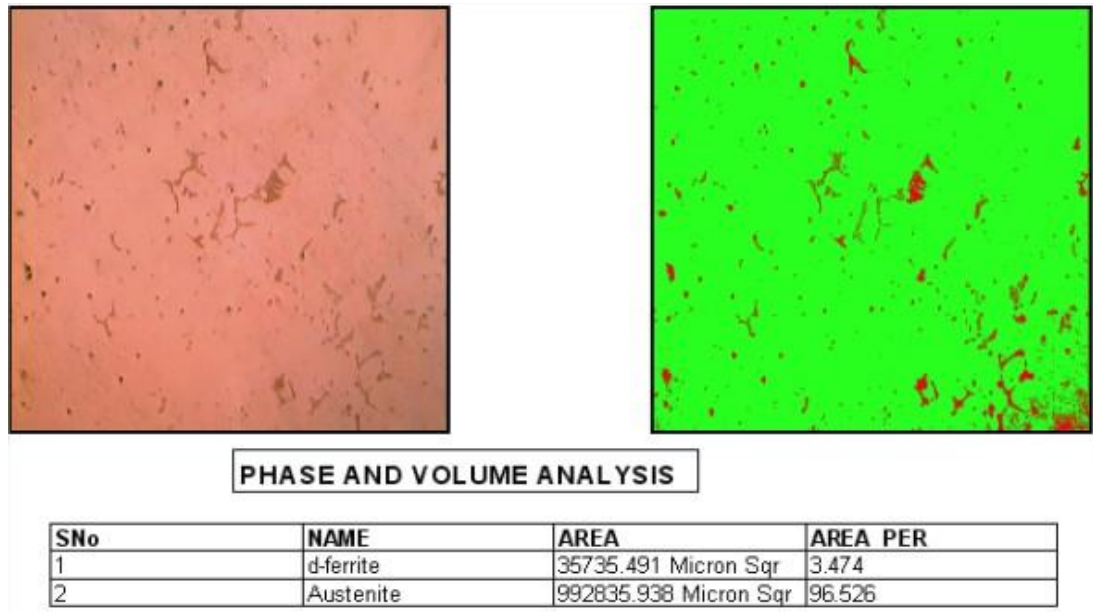


**Figure 4.1** Metallographic image analysis result of AND-5 Steel.

Phase analysis results confirmed the measurements carried out with feritscope® for steel 5. Delta ferrite content of steel 5 is found in a range of 1 – 4 % with both methods. Furthermore these results are also confirmed the estimations made by the ORNL constitution diagram. Chromium and nickel equivalents of Steel 4 and steel 5 based on equations 2.10 and 2.11 are written as follows:

For Steel 4;

$$Cr_{eq}: 25.46$$

$$Ni_{eq}: 13.3644$$

For Steel 5;

$Cr_{eq}$ : 28.3525

$Ni_{eq}$ : 21.749

Finally, 3 determination methods, which confirm each other in terms of delta ferrite percentages, are used to obtain delta ferrite contents of candidate steels used in this study. Delta ferrite contents of steel 4 and steel 5 are measured by Metallographic image analysis and Feritscope<sup>®</sup> methods and they have confirmed each other. Furthermore, figure 4.2 represents the estimation of delta ferrite content of steel 4 and steel 5. According to the estimations, d-ferrite content of the exact composition of steel 5 is around 2.5 % while that of steel 4 (316L) is around 3.6 % which are also confirmed by other 2 methods.

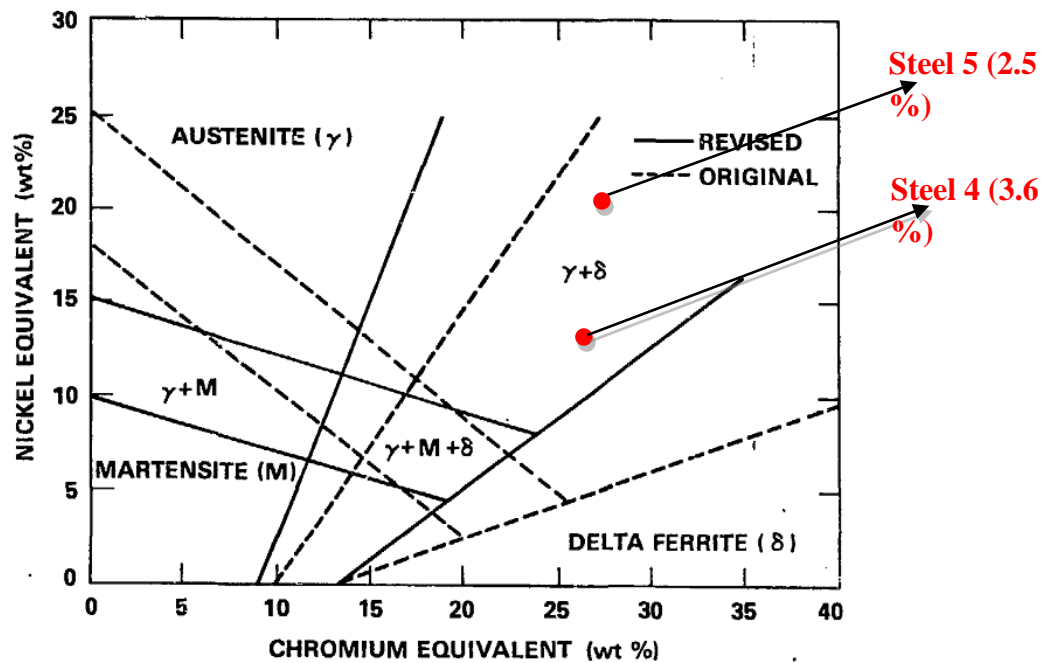


**Figure 4.2** Delta ferrite estimation of Steel 4 and 5 according to ORNL Diagram.

## 4.2. Characterization of Galvanizing Bath

In order to verify that galvanizing media is obtained in the immersion corrosion tests of this study, galvanizing bath is prepared carefully and alloyed precisely to the standard levels. It can be said that simulation of galvanizing bath is achieved when chemical composition and morphology of the coating is attained. In line with this purpose, chemical composition of the galvanizing bath used in this study is measured both with spectrometer and EDS unit of SEM. In addition, coating morphology is imaged using SEM. Table 4.2 shows one of the daily spectral analysis results carried out with spectrometer for the purpose of maintaining the galvanizing bath composition at limits of galvanizing.

**Table 4.2** Typical chemical composition of galvanizing bath.

<b>Al</b>	<b>Cu</b>	<b>Fe</b>	<b>Pb</b>	<b>Ag</b>	<b>Cd</b>	<b>Mg</b>
<b>0.1837</b>	0.0170	0.0178	0.0280	0.0018	0.0087	<0.0010
<b>Mn</b>	<b>Ni</b>	<b>Sb</b>	<b>Sn</b>	<b>Ti</b>	<b>Cr</b>	<b>Zn</b>
<b>0.0027</b>	0.0210	0.0878	0.916	<0.0050	0.495	Remainder

Coating morphology is also observed with SEM as shown in figure 4.3. As expected from a galvanizing media containing aluminum higher than 0.14 wt. %, ternary phase  $\eta$  formation with a non-uniform thickness is observed. According to the EDS analyses results, this thin, ternary alloy consist of Fe, Zn and Al with a stoichiometry of  $Fe_2Al_{5-x}Zn_x$  [32, 33]. Figure 4.4 shows the EDS Analyses results taken from the interface of the coating where ternary  $Fe_2Al_{5-x}Zn_x$  phase formed. In table 4.3, weight and atomic percentages of  $Fe_2Al_{5-x}Zn_x$  phase is seen.

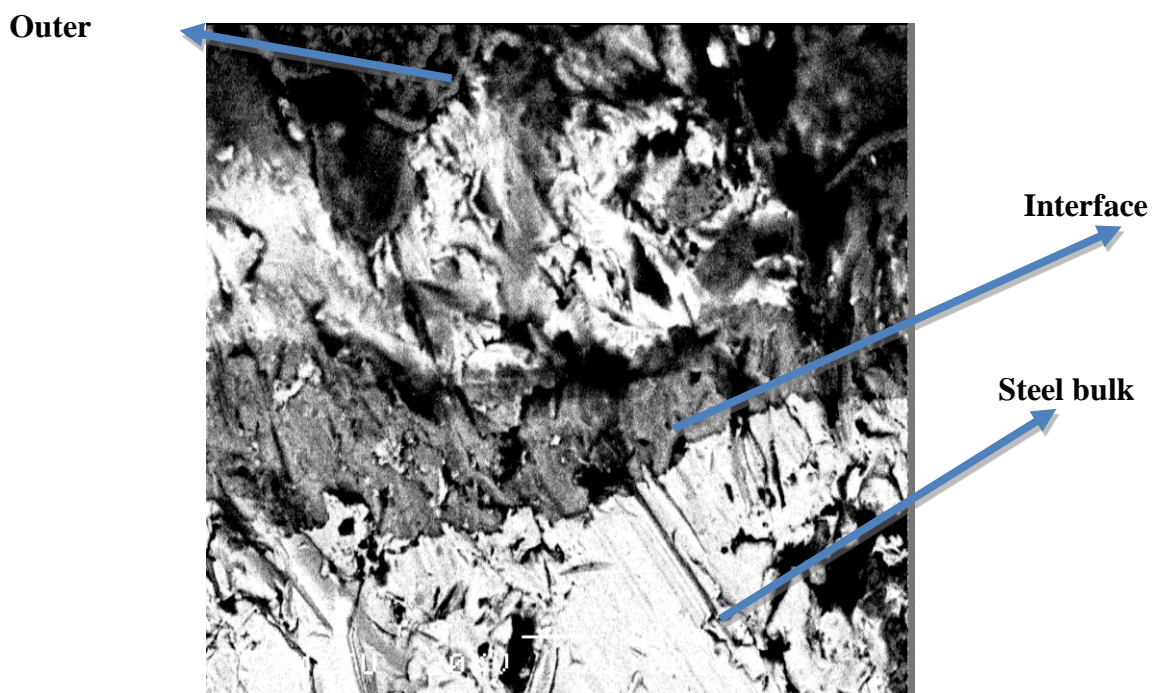


**Figure 4.3** Cross sectioned SEM image of galvanize coating (BS).

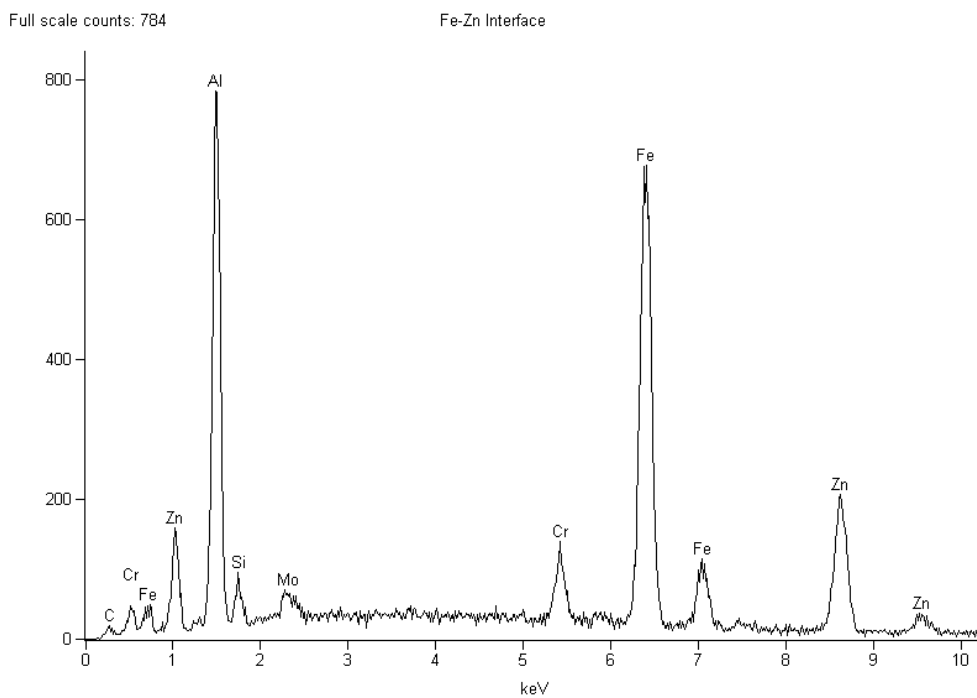


**Figure 4.4** EDS analysis pattern for stainless steel – coating interface where  $\text{Fe}_2\text{Al}_5\text{-}_x\text{Zn}_x$  formation is observed.

**Table 4.3** Chemical composition of eta ( $\eta$ ) phase in atomic and weight percent.

<i>Element</i>	<i>Weight Conc %</i>	<i>Atom Conc %</i>
<i>Al</i>	24.45	41.00
<i>Si</i>	2.04	3.29
<i>Cr</i>	3.54	3.08
<i>Fe</i>	41.04	33.24
<i>Zn</i>	26.14	18.08
<i>Mo</i>	2.80	1.32

As can be seen from table 4.3, chemical composition of ternary alloy layer coincides with the stoichiometry of  $Fe_2Al_{5-x}Zn_x$  phase in terms of atomic and weight percentages. These results also match closely with the ones found from literature [21, 25, 32, 33]. Zhang et al. [6] found  $Fe_2Al_{5-x}Zn_x$  phase containing approximately 50.2 atomic % Al, 28.8 % Fe, 19.3 Zn, 1.1 % Mo and 0.6 % Cr. Slight difference between diffusion kinetics of two galvanizing baths blocks the exact matching of chemical compositions of eta phases of these two studies [6].

Similar to the stainless steel – coating interface morphology, chemical compositions of outer surface of the galvanized samples were found very close to the ones found from literature. Figure 4.5 and table 4.4 contains chemical composition results of outer layer of coating.

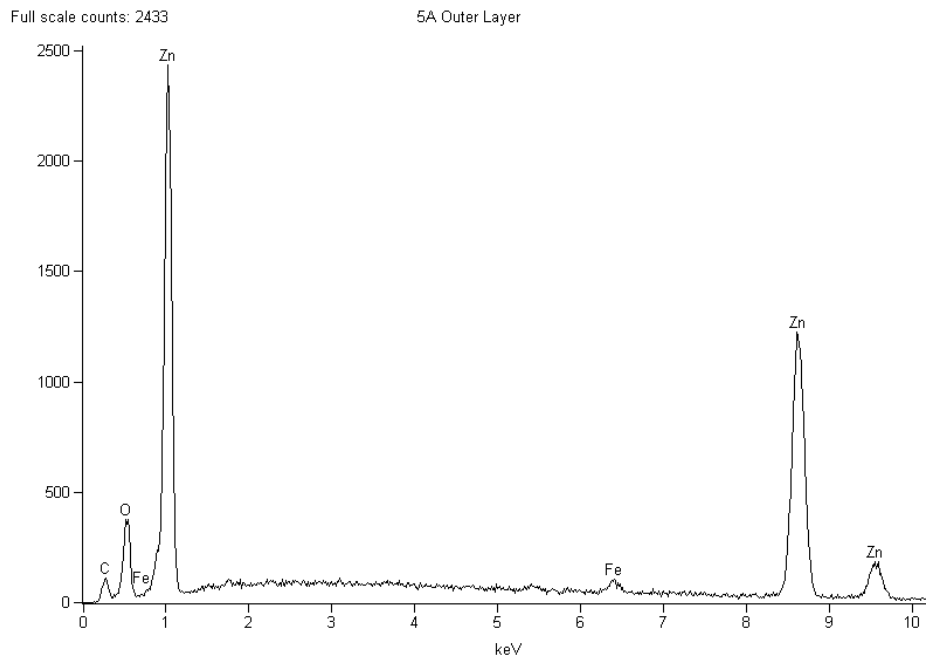


**Figure 4.5** EDS analysis pattern for outer layer of stainless steel – coating.

Slight diffusion of Fe to zinc coating is observed on EDS pattern of outer layer as expected from a typical galvanized coating[20].FeZn<sub>13</sub> and pure zinc phases are present in this region where the weight percentage of iron is approximately 2 %. These phases appeared darker than Fe-Al-Zn phase as can be seen from figure 4.3.

**Table 4.4** Chemical compositions of outer layer of coating in atomic and weight percent.

<i>Element</i>	<i>Weight Conc %</i>	<i>Atom Conc %</i>
<b><i>Fe</i></b>	1.80	2.10
<b><i>Zn</i></b>	98.20	97.90

By evaluating the results of SEM-EDS techniques and that of spectral analyses, it can easily be concluded that typical galvanizing environment is achieved in this set of materials. Coating morphology and chemical composition of the phases formed on the samples verify with the ones found from literature as well as the spectral analyses carried out to the samples which were periodically taken from galvanizing bath.

### **4.3. Immersion Corrosion Test Results & Corrosion Rates**

Corrosion performance of a sink roll is crucial in practice for the reason that the corrosion damage on its surface causes shadows, marks etc. on the coating of steel strip. Marked or damaged strip cannot be used in any application so this is unacceptable for a continuous galvanizing line. In order to prevent marks or shadows on the steel strip to be coated, sink roll is taken from the bath for maintenance. During maintenance, firstly, zinc is removed via acid pickling. Following acid pickling, sink roll is turned in order to make its surface smooth and clear. Finally it is heated to galvanizing bath temperature and got into use again until its wall thickness decreases to a certain level. Whole this maintenance procedure brings additional and significant costs to galvanizing line because of the unplanned stoppage of coating process. In this set of materials, corrosion performance of the steel grade to be used as sink roll material is critical. Enhancing corrosion performance of a sink roll would increase the efficiency of the continuous galvanizing line extremely.

In this set of experiments, firstly weight loss of 20 corrosion specimens are measured after immersion of them into the galvanizing bath. 5 of them (1 set) are taken from the bath after 168 hours while others are taken after 504 hours. Table 4.5 summarizes initial weights, final weights and mass losses of the specimens exposed for 504 hours due to molten metal corrosion. Furthermore, comparisons of weight losses for different time intervals are seen in Table 4.6.

**Table 4.5** Mass loss values of corrosion specimens.

<b>Specimen</b>	<b>Initial weight (g)</b>	<b>Final Weight (g)</b>	<b>Mass Loss (g)</b>
<b>1A</b>	38.5776	30.2342	8.3434
<b>2A</b>	39.8058	33.9840	5.8218
<b>3A</b>	38.3418	33.1742	5.1676
<b>4A</b>	39.4163	17.4220	21.9943
<b>5A</b>	39.3753	33.3977	5.9776
<b>1B</b>	39.4778	34.9911	4.4867
<b>2B</b>	38.3716	34.1632	4.2084
<b>3B</b>	38.9552	35.0178	3.9374
<b>4B</b>	38.7118	33.8060	4.9058
<b>5B</b>	39.8447	35.1944	4.6503
<b>1C</b>	39.7781	33.5584	6.2197
<b>2C</b>	39.2724	34.7589	4.5135
<b>3C</b>	40.3745	34.0510	6.3235
<b>4C</b>	37.9908	32.5038	5.487
<b>5C</b>	39.3201	33.2526	6.0675
<b>1D</b>	39.1822	32.7530	6.4292
<b>2D</b>	39.588	34.4128	5.1752
<b>3D</b>	38.7779	33.2553	5.5226
<b>4D</b>	39.1806	33.6044	5.5762
<b>5D</b>	40.0642	33.0188	7.0454

In table 4.5, four set of specimens can be seen each of which have different heat treatment condition or exposure time. Each set consist of 5 specimens and every one of them represents one candidate steel for instance specimen 4C represents steel 4 (AISI 316L) with heat treatment condition of solution treatment and exposure interval of 504 hours. Similarly, specimen 1A represents steel 1 with heat treatment

condition of Age treated at 750 °C and exposure interval of 504 hours. Table 3.2 in section 3.3.2 gives more detailed information.

**Table 4.6** Weight loss comparison at different time intervals.

<b>Specimen</b>	<b>Initial Weight (g)</b>	<b>Final Weight (g)</b>	<b>Mass Loss (g)</b>	<b>Mass loss Difference (%)</b>
<b>1B</b>	39.4778	34.9911	4.4867	11.36
<b>2B</b>	38.3716	34.1632	4.2084	10.96
<b>3B</b>	38.9552	35.0178	3.9374	10.10
<b>4B</b>	38.7118	33.8060	4.9058	12.67
<b>5B</b>	39.8447	35.1944	4.6503	11.67
<b>1C</b>	39.7781	33.5584	6.2197	15.63
<b>2C</b>	39.2724	34.7589	4.5135	11.49
<b>3C</b>	40.3745	34.0510	6.3235	15.66
<b>4C</b>	37.9908	32.5038	5.487	14.44
<b>5C</b>	39.3201	33.2526	6.0675	15.43

As for table 4.6, set B has an exposure time of 168 hours while set C has 504 hours. This difference leads specimens of set C to corrode more than that of set B. Although set C has been exposed to the galvanizing media 3 times longer than set B, mass loss difference between them is not linear; it is approximately 5 %. The reason for these results is that corrosion products slowly cover up surfaces of specimens thus slow down the acceleration of corrosion. In practice, corrosion products go away as the sink roll rotates to pass the steel strip to be coated. It can be said that mass loss difference for different time intervals would be higher than these results in dynamic conditions. Further results such as corrosion rate, mass loss per unit area can be seen on table 4.7.

**Table 4.7** Corrosion rates & mass loss per unit area values for corrosion specimens.

<b>Specimen</b>	<b>Surface Area (mm<sup>2</sup>)</b>	<b>Mass loss per unit area (mg/mm<sup>2</sup>)</b>	<b>Corrosion Rate x 10<sup>4</sup> (g/cm<sup>2</sup>h)</b>
1A	3017.664	2.7649	5.4858
2A	3027.472	1.9230	3.8155
3A	3007.356	1.7183	3.4094
4A	3025.96	7.2685	14.4217
5A	3025.463	1.9758	3.9202
1B	3026.469	1.4825	8.8243
2B	3011.374	1.3975	8.3185
3B	3009.871	1.3082	7.7867
4B	3018.42	1.6253	9.6743
5B	3032.501	1.5335	9.1279
1C	3025.96	2.0554	4.0783
2C	3018.42	1.4953	2.9669
3C	3033.759	2.0844	4.1357
4C	3016.653	1.8189	3.6089
5C	3021.186	2.0083	3.9848
1D	3030.497	2.1215	4.2093
2D	3030.497	1.7077	3.3883
3D	3023.195	1.8267	3.6245
4D	3020.425	1.8462	3.6630
5D	3030.243	2.3250	4.6132

Corrosion rate on table 4.7 is calculated with the equation 3.1 as follows:

$$\text{Corrosion rate} = (K \times W) / (A \times T \times D)$$

Since constant  $K = 1 \times D$ ;

$$\text{Corrosion Rate} = 1 \times D \times W / A \times T \times D \quad \text{and};$$

$$\text{Corrosion rate} = W / A \times T$$

Where:

T= time of exposure in hours

A= surface area in  $\text{cm}^2$

W= mass loss in grams

From table 4.7, it is seen that aging treatment (16 hours at 750 °C) does not affect the corrosion rates of steels significantly. There are only slight differences between aged and non-aged specimens (set A is aged while sets C and D are not). For steels 1, 2, 3 and AISI 316L, corrosion rates and mass loss per unit area values are slightly greater in aged specimens in comparison to non-aged ones. In contrast to other candidate steels, aged specimens of steel 5 have corroded at lower levels when compared with non-aged ones. These results could make difference in practice (usage of these steels as sink rolls or other galvanizing bath hardware whether aged or not) in terms of corrosion performance but one must evaluate both corrosion and mechanical performance before making a decision. Parallel with mass loss results, mass loss per unit area values of set B, which are immersed into bath for 7 days (168 hours), are lower than that of other sets which are immersed into bath for 21 days (504 hours). On the contrary, corrosion rates of set B are way much higher than that of other sets since corrosion takes place immediately after the steel is immersed into the bath, then slows with the deposition of dross onto specimens [18, 20].

Based on the corrosion results for 5 different candidate steels, generally steel 2 and AISI 316L performed better than other candidates in solution annealed condition for 504 hours. In shorter exposure time, AISI 316L corroded the most as well as in its aged condition. Higher delta ferrite content of AISI 316L leads to sigma and chi ( $\chi$ ) phase formation and so severe dissolution is observed in its aged condition as can be seen from corrosion rates of specimen 4A. More than 50 % of its initial mass has been lost during immersion corrosion tests since delta ferrite phase preferentially dissolves before austenite in galvanizing media [36-38].

Steel 2, steel 3 and steel 5 showed stable corrosion performance at different heat treatment regimes. Among them, steel 2 has showed the best corrosion performance while steel 3 is superior to steel 5. According to the visual inspection of corroded specimens, roughness of the specimens of steels 1, 2, 3 and 4 were almost the same while specimens of steel 5 has smoother and cleaner surfaces which is an important advantage in service conditions. When sink roll surface becomes rough, it marks the steel strip to be coated and this causes unplanned line stoppages. For this reason, smoothness of the surface is dramatically important even if the steel in subject corrodes more than its alternatives. Figure 4.6 shows the actual photograph of specimens 4A (AISI 316L) and 5A both of which are aged at 750 ° C and immersed into the galvanizing bath.



**Figure 4.6** Corrosion tested condition of specimens 4A (black one) and 5A.

It is obviously seen that AISI 316L steel is suffered from pitting corrosion at extreme levels in comparison to steel 5. Almost its entire surface is destroyed because of molten metal corrosion along with pitting corrosion in galvanizing media. In practical conditions, such damage can obstruct the function of sink rolls and in those conditions sink roll needs to be maintained immediately. This maintenance results in line stoppage and increases running cost of continuous galvanizing line dramatically.

#### **4.4. Mechanical Testing Results**

In mechanical testing stage of this study, series of tensile and v-notch charpy impact tests are carried out to 5 candidate steels at different heat treatment and/or aging conditions. Table 3.3 in section 3.1.1 shows 4 different heat treatment regimes applied to mechanical testing specimens. Subsequent to heat treatment operations, mechanical tests are conducted and results of each candidate steels are given separately as follows while all of the results are discussed in section 4.4.6.

##### **4.4.1. Steel 1**

Steel 1 contains high manganese and high chromium and relatively low nickel for the purpose of maintaining its almost full austenitic microstructure as well as corrosion resistance. It is a widely known fact that Nickel is an expensive alloying element; thus it is aimed to replace it with manganese since it is also a strong austenite promoter in steels. Additionally, nitrogen for pitting corrosion resistance and creep resistance, wolfram, and vanadium for creep resistance are also microalloyed to steel 1 [10]. Tensile and charpy impact testing results for steel 1 are seen in table 4.8.

**Table 4.8** Mechanical tests results of steel 1

<b>Condition</b>	<b>Tensile Strength (MPa)</b>	<b>Yield Strength (MPa)</b>	<b>Elongation (%)</b>	<b>Reduction of Area (%)</b>	<b>Impact Energy (J)</b>
<b>Solution annealed</b>	591	164	51.8	47	208
<b>Exposed to 460 ° C</b>	702	182	54.8	53.5	38
<b>Aged at 750 ° C</b>	524	165	9.72	3.14	3
<b>Aged at 750 ° C then Exposed to 460 ° C</b>	529	201	11.22	3.13	3

**4.4.2. Steel 2**

Steel 2 is a high chromium and nickel steel with relatively high microalloy content when compared with other candidate steels. Extremely low carbon content of steel 2 is drawing attention. Naturally, this brings it a very high level of toughness while precipitates of microalloying elements such as vanadium nitride increase its strength. Results of mechanical testing for steel 2 are seen on Table 4.9.

**Table 4.9** Mechanical tests results of steel 2

<b>Condition</b>	<b>Tensile Strength (MPa)</b>	<b>Yield Strength (MPa)</b>	<b>Elongation (%)</b>	<b>Reduction of Area (%)</b>	<b>Impact Energy (J)</b>
<b>Solution annealed</b>	505	141	73.58	82.7	286

**Table 4.9** Mechanical tests results of steel 2 (continued)

<b>Exposed to 460 ° C</b>	<b>586</b>	<b>153</b>	<b>65.61</b>	<b>70.34</b>	<b>205</b>
<b>Aged at 750 ° C</b>	528	179	47.5	33.11	32
<b>Aged at 750 ° C then Exposed to 460 ° C</b>	540	152	50.84	31.76	31

#### 4.4.3. Steel 3

Steel 3 is a modified version of AISI 316L, with its additional manganese and microalloying content. Silicon content is reduced and also manganese is alloyed to steel 3 in order to reduce delta ferrite content thus suppress detrimental effects of it. Microalloying elements are alloyed for the purpose of increasing creep strength. It has also extremely low carbon content which makes it tougher similar to steel 2. Table 4.10 gives mechanical properties of steel 3 obtained from tensile and impact tests.

**Table 4.10** Mechanical tests results of steel 3

<b>Condition</b>	<b>Tensile Strength (MPa)</b>	<b>Yield Strength (MPa)</b>	<b>Elongation (%)</b>	<b>Reduction of Area (%)</b>	<b>Impact Energy (J)</b>
<b>Solution annealed</b>	505	141	73.58	82.7	286
<b>Exposed to 460 ° C</b>	586	153	65.61	70.34	205
<b>Aged at 750 ° C</b>	528	179	47.5	33.11	32

**Table 4.10** Mechanical tests results of steel 3(continued)

<b>Aged at 750 ° C then Exposed to 460 ° C</b>	<b>540</b>	<b>152</b>	<b>50.84</b>	<b>31.76</b>	<b>31</b>
--	------------	------------	--------------	--------------	-----------

**4.4.4. Steel 4 (AISI 316L)**

AISI 316L is the most common steel grade used in fabrication of galvanizing bath hardware such as sink rolls, correcting rolls and stabilizing rolls. As a consequence, it is an important candidate steel since this study interests in galvanizing bath hardware materials. Results of the centrifugal cast AISI 316L steel used in study are given in table 4.11.

**Table 4.11** Mechanical tests results of AISI 316L.

<b>Condition</b>	<b>Tensile Strength (MPa)</b>	<b>Yield Strength (MPa)</b>	<b>Elongation (%)</b>	<b>Reduction of Area (%)</b>	<b>Impact Energy (J)</b>
<b>Solution annealed</b>	704	247	43.82	58.9	170
<b>Exposed to 460 ° C</b>	968	218	26.94	10.22	8
<b>Aged at 750 ° C</b>	294	136	2.77	1.16	2
<b>Aged at 750 ° C then Exposed to 460 ° C</b>	395	154	3.83	1.31	2

#### 4.4.5. Steel 5

Steel 5 has high carbon and nickel levels as compared to other candidate steels. It seems to have the same chemical composition with steel 2 but in fact contents of critical microalloying elements such as nitrogen and vanadium distinguish them as well as carbon and nickel content. Table 4.12 contains mechanical testing results for steel 5.

**Table 4.12** Mechanical tests results of AISI 316L.

<b>Condition</b>	<b>Tensile Strength (MPa)</b>	<b>Yield Strength (MPa)</b>	<b>Elongation (%)</b>	<b>Reduction of Area (%)</b>	<b>Impact Energy (J)</b>
<b>Solution annealed</b>	628	166	43.82	75.8	150
<b>Exposed to 460 ° C</b>	655	177	26.94	71.06	78
<b>Aged at 750 ° C</b>	535	152	2.77	30.91	11
<b>Aged at 750 ° C then Exposed to 460 ° C</b>	572	174	3.83	33.29	16

#### 4.4.6. Discussion of Mechanical Testing Results

From the mechanical testing results, especially from charpy impact results, it is clearly seen that all 5 candidate steels have lost their toughness after a typical galvanizing heat treatment condition which lasts 21 days at 460 °C. Reduction in toughness not only causes fissures in welded areas such as flanges or necks of sink rolls but also results in fracture of bearings and locking rotation of sink rolls even if

the stress applied on sink rolls are relatively low for stainless steels. For these reasons, a stainless steel which has high temperature strength without losing its toughness is aimed for fabrication of a sink roll. If the steel is too ductile, its high temperature strength will be low thus it will suffer from creep. Consequently, the deflection caused by creep will affect the rotation of sink roll and smoothness of steel strip to be coated. In these conditions sink roll must be taken out from the galvanizing bath for maintenance.

As for the typical galvanizing regime which is 21 days (504 hours) at approximately 460 °C, Charpy impact value of the steels used in this study has reduced extremely. According to the impact testing results for steel 1, it has lost 78.5 % of its toughness while steel 2, steel 3, steel 4 and steel 5 have lost 28.3, 29.8, 95.3 and 48 % respectively. In actual working conditions, loss of toughness renders them to have poor resistance to cracking at service conditions. It is observed that toughness loss values of Steel 2, Steel 3 and steel 5 are lower than steel 1 and steel 4 (AISI 316L) which makes them superior in terms of mechanical properties. According to the results of tensile tests, all candidate steels have maintained their elongation and reduction of area values except AISI 316L. It has shown brittle behavior due to the sensitization caused by higher delta ferrite content in it. It can be said that steels 2, 3 and 5 are good candidates to select as sink roll material in a mechanical way since AISI 316L has lost 95 % of its initial impact energy and 82.6 % of its initial reduction of area while they have maintained at least 50 % of their impact energy and almost all of their reduction of area values. AISI 316L has shown complete brittle behavior after galvanizing regime; tensile strength has increased by 28 %, yield strength has decreased by 37.6 %, elongation has decreased by 38.52 % along with its toughness. It is obvious that steels 2, 3 and 5 are better than AISI 316L in terms mechanical properties for typical galvanizing regimes. The reason for this difference between them is the delta ferrite content of AISI 316L is higher unlike the other candidates and also it does not contain microalloying elements such as vanadium which acts as a stabilizer element. Vanadium precipitates with N and C before any other element in steel and exhibits fine precipitation. Thus, it not only helps avoiding

sensitization but also increases high temperature strength and creep strength of stainless steels as a microalloying element [54]. One other reason of higher mechanical properties of steels 2, 3 and 5 is higher nitrogen content of them. Nitrogen is a strong austenite stabilizer therefore it reduces the delta ferrite content of stainless steel. Besides this, it increases strength of the steel when it is uniformly distributed to the microstructure of it [73].

Materials are also tested at two other heat treatment regimes. One of these two regimes is aging at 750 °C for 16 hours in order to combine vanadium with carbon and nitrogen. Other one consists of two stages, one of which is aging at 750 °C and the other one is exposing materials to a typical galvanizing regime for galvanizing bath hardware (504 hours at 460 °C). From the mechanical testing results of these series, it is obviously seen that the entire candidate steels have lost their mechanical properties dramatically. Steel 2 has shown best performance among 5 steels nonetheless it has also lost its toughness by 89.2 % whilst AISI 316L has shown the worst performance with a toughness reduction of 99 %. The reason for this loss of mechanical properties can be explained by the formation of sigma phase. Table 4.13 gives the equivalent chromium content (see equation 2.12) values of 5 steels used in this study.

**Table 4.13** Equivalent Chromium Contents of 5 Candidate Steels

<b>Steel No</b>	<b>ECC</b>
<b>1</b>	29.34
<b>2</b>	26.03
<b>3</b>	24.43
<b>4 (AISI 316L)</b>	23.42
<b>5</b>	25.45

At temperatures above 540 °C, ferrite phase in stainless steels can transform to sigma phase. Austenite can also transform to sigma phase directly. Sigma phase formation is seen in steels which have equivalent chromium content (ECC) higher than 17 – 18 %. As it can be seen on table 4.11, ECC of the stainless steels used in this study have 23.42 to 29.34. In this set of materials, it can be concluded that aging treatment at 750 °C caused sigma phase formation in the candidate steels and they have lost almost all of their initial toughness and ductility. In conclusion, even if the aging treatment at 750 °C would be successful to combine vanadium with carbon and nitrogen, it has failed to enhance mechanical properties of these alloys since sigma phase formation extremely reduced their toughness [67, 74].

Finally, in absence of corrosion related problems, steel 2 and steel 5 have the optimum mechanical properties to be used in fabrication of sink rolls or other galvanizing bath hardware such as correcting rolls or stabilizing rolls.

## **CHAPTER 5**

### **CONCLUSIONS**

The main objective of this thesis study was to investigate corrosion behaviors of 4 new developed and 1 commonly used stainless steels to be used in fabrication of sink rolls, which possess one of the most critical function in continuous galvanizing lines, in specific galvanizing media consisting of 0.14 – 0.21 weight percent aluminum. After conducting series of experiments involving conditioning with heat treatment, tensile and v-notch impact tests, immersion corrosion tests and characterization of galvanizing media and coating with SEM, corrosion and mechanical performance of these steels are discussed depending on their service conditions. Considering the fact that delta ferrite phase in austenitic stainless steels strongly affects their corrosion and mechanical performance in service conditions, delta ferrite content of candidate stainless steels are determined with 3 different methods and its effect on results are also discussed.

In practice, a sink roll should pass as much as steel strip from galvanizing bath without causing any mark on strip, slippage, locking of line, vibration, or waving. Steel grade used in production of a sink roll must have certain properties to accomplish this purpose. It has to be corrosion resistant in order not to mark the steel strip passing on. Locking of line, vibration and/or waving depend on the runout level of sink roll. In an effort to prevent runout, steel must have high temperature strength as well as creep strength (note that using steel which have excessively high levels of strength can also mark the strip to be coated). In order to test these features of 5

different stainless steels, 4 of which are newly designated, series of experiments were conducted and results are given and discussed as follows:

- I. It is a well-known fact that delta ferrite in stainless steels strongly decreases their corrosion performance since it leads to sensitization hence sigma and chi phase precipitation, both of which lowers steels toughness and corrosion resistance. One method for determination of delta ferrite is not sufficient because any of these methods are not capable of providing 100 % true results. Therefore 1 constitution diagram, 1 non-destructive and 1 destructive method are used to determine delta ferrite content of candidate steels. It is found that 3 methods chosen from 6 of them are confirmed each other closely. As for the effect of delta ferrite on corrosion and mechanical properties of alloys, it is seen that both corrosion and mechanical performance of AISI 316L turned out to be the worst of 5 steels because of its higher delta ferrite content.
- II. Mechanical tests are carried out at 4 different heat treatment conditions. From mechanical testing results, it can be concluded that all of 5 candidate steels are greatly affected from typical galvanizing regimes. Mechanical properties such as tensile and yield strength, elongation, reduction of area and impact energy values of steels 2 and 5 are reasonable while steel 1 and AISI 316L are embrittled enormously. Aging treatment at 750 ° C in order to provide fine precipitation of carbides and nitrides is failed to improve mechanical properties of these steels.
- III. Corrosion testing of this study involved immersion corrosion tests for 168 hours and 504 hours in a specific galvanizing bath. Results indicated that corrosion rates of specimens are not linear to the immersion period because corrosion products cover surface of steel quickly and slow the acceleration of corrosion reaction. It is seen that aging did not affect corrosion rates and mass loss per unit area values of these steels except AISI 316L. Due to its high delta ferrite level, 316L specimen in aged condition has lost more than 50 % of its initial mass. Based on the corrosion rates of specimens for a typical galvanizing regime of a sink roll, which is 21 days in galvanizing bath, steel 2 and AISI 316L have shown lower values than that of steel 1, 3 and 5. However, visual inspections of corroded specimens have lead different

decisions. Steel 5 had the most clean and smooth surface among 5 candidate steels even though its corrosion performance was worse than steel 2.

IV. Based on the combination of immersion corrosion and mechanical testing results, steel 2 and steel 5 are chosen to be the best 2 steels from 5 candidate steels investigated in this study. Steel 3 has a performance which is closer to steel 2 and 5 while steel 1 and steel 4 (AISI 316L) has weak performance in comparison to other steels.

In order to have a better aspect and understanding of performance of these steels, testing should continue and following studies should be done in future:

1. Extensive characterization methods should be applied on candidate steels on purpose of understanding their microstructures.
2. Immersion corrosion tests should be tried in dynamical conditions since actual sink rolls works in these conditions.
3. Optimization of aging treatment should be carried out and improvement of mechanical properties of these alloys under favor of fine precipitated microalloying compounds such as VN, VC etc.
4. Coating morphologies of all of these steels should be studied in order to extract information regarding adhesion of coating to steel surface.

## REFERENCES

1. *World Directory: Continuous Galvanizing Lines 2010*. 2010, International Lead and Zinc Study Group: Lisbon. p. 9 - 77.
2. Bright, M.A., *Dissolution and Diffusion Characteristics of 316L Stainless Steel in Molten Zinc Containing Variable Concentrations of Aluminum*, in *Mechanical Engineering*. 2007, West Virginia University: Morgantown. p. 4-36.
3. Brunnock, M.S. and e. al., *Interactions between liquid zinc and bath hardware materials in continuous galvanising lines* *Ironmaking and Steelmaking*, 1996. **23**(2): p. 171 - 176.
4. Brunnock, M.S. and e. al., *Supermeniscus Interactions Between Molten Zinc and Bath Hardware Materials In Galvanizing*. *Ironmaking and Steelmaking*, 1997. **24**(1): p. 40 - 46.
5. Xu, J., et al., *Liquid Metal Corrosion of 316L Stainless Steel, 410 Stainless Steel, and 1015 Carbon Steel in a Molten Zinc Bath*. *Metallurgical and Materials Transactions A*, 2007. **38A**: p. 2727 - 2736.
6. Zhang, K., et al., *Reaction of 316L Stainless Steel with a Galvanizing Bath*. *Journal of Materials Science*, 2007. **42**: p. 9736-9745.
7. Sikka, V., F.E. Goodwin, and K.-M. Chang. in *Galvanizer's Association Meeting*. 2002. Dearborn, MI.
8. Sikka, V., et al., *DOE-OIT Project: Development of Improved Materials for Pot Hardware*. 2005.
9. *Metals Handbook*. 10th ed. Vol. 1. March 1990, Materials Park, OH.: ASM International.

10. Davis, J.R., *ASM Specialty Handbook: Stainless Steels*. 1994: ASM International. 3-66.
11. Peckner, D. and I.M. Bernstein, *Handbook of Stainless Steels*. 1977: McGraw- Hill.
12. Sedricks, A.J., *Corrosion of Stainless Steels*. 1979: John Wiley and Sons.
13. S.D Washko and G. Aggen, *Wrought Stainless Steels, Properties and Selection: Irons, Steels and High-Performance Alloys*. 1990. **1**: p. 841-907.
14. Khatak, H.S. and B. Raj, *Corrosion of austenitic stainless steels : mechanism, mitigation and monitoring*  
2002: Woodhead publishing.
15. Rula, R.A., *Stainless Steel*. 1986: American Society For Metals.
16. Potts, D.L. and J.G. Gensure, *International Metallic Materials Cross Reference*. 1989: Genium Publishing.
17. Brown, R.S., *How to Select the Right Stainless Steel*. *Advanced Materials & Processes*, 1994.**4**(45): p. 20-24.
18. Dallin, G.W., *Hot-Dip Coated Sheet Products*, in *Metallic Coated Products and Specifications*. Jan. 2011, International Zinc Association.
19. Maaß, P. and P. Peißker, *Handbook of Hot-dip Galvanization*. 1 ed. 2011: Wiley-VCH.
20. Dallin, G.W., *Continuous Hot-Dip Galvanizing versus General (Batch) Galvanizing*, in *Coating Processes and Surface Treatments*. Jan. 2011, International Zinc Association.
21. Dallin, G.W., *Galvanneal – Differences from Galvanize*, in *Metallic Coated Products and Specifications*. Jan. 2011, International Zinc Association.
22. Dallin, G.W., *55% Aluminum-Zinc Alloy-Coated Steel Sheet*, in *Metallic Coated Products and Specifications*. Jan. 2011, International Zinc Association.
23. Carlsson, P. (2005) *Surface Engineering in Sheet Metal Forming*. **Volume**, 7-9
24. Selverian, J.H., A.R. Marder, and M.R. Notis, *The Effects of Silicon on the Reaction Between Solid Iron and Liquid 55 wt. % Al-Zn Baths* *Metallurgical Transactions*, 1989. **20A**: p. 543-555.

25. Marder, A.R., *The Metallurgy of Zinc-Coated Steel*. Progress in Materials Science, June 2000. **45**(3): p. 229-232.
26. Weinberg, F., M. Mager, and L. Frederick, *Segregation in Galvan Hot Dipped Sheet Steel*. Canadian Metallurgical Quarterly, 1990. **29**(2): p. 163-166.
27. Dallin, G.W., *Zinc-5% Aluminum Alloy-Coated Steel Sheet*, in *Metallic Coated Products and Specifications*. Jan. 2011, International Zinc Association.
28. Goodwin, F.E. and R.N. Wright. *The Process Metallurgy of Zinc-Coated Steel Wire and Galvan® Bath Management*. in *Wire & Cable Technical Symposium*. 2001. Guilford CT: The Wire Association International Inc.
29. Chavan, R.R., *Analysis of Energy Consumption in Continuous Galvanizing Lines*, in *Industrial Engineering*. 2006, West Virginia University: Morgantown. p. 5.
30. Brunnock, M.S. and e. al. *Durability of bath hardware materials in continuous galvanizing*. in *1996 Galvanizers Association*. 1996. Chicago, IL.: Galvanizers Association.
31. Irwin, C., et al., *DOE-OIT Project: Development of Improved Materials for Pot Hardware*. June 2005.
32. Dallin, G.W., *The Role of Aluminum in Continuous Hot-Dip Galvanizing*, in *Coating Processes and Surface Treatments*. Jan. 2011, International Zinc Association.
33. Dallin, G.W., *Zinc Bath Management on Continuous Hot-Dip Galvanizing Lines*, in *Coating Processes and Surface Treatments*. Jan. 2011, International Zinc Association.
34. Bright, M.A., *Dissolution and Diffusion Characteristics of 316L Stainless Steel in Molten Zinc Containing Variable Concentrations of Aluminum*, in *Mechanical Engineering*. 2007, West Virginia University: Morgantown. p. 4-36.
35. Tang, N.-Y., *Determination of liquid-phase boundaries in Zn-Fe-Mx systems* Journal of Phase Equilibria, 2000. **21**: p. 70-77.
36. Tverberg, J.C., *The Role of Alloying Elements on the Fabricability of Austenitic Stainless Steel*. February 2003.

37. Prager, M., *Cast High Alloy Metallurgy, Steel Casting Metallurgy*. 1984: Steel Founders' Society of America. 221 - 245.
38. Bates, C.E. and L.T. Tillery, *Atlas of Cast Corrosion-Resistance Alloy Microstructures*. 1985: Steel Founders' Society of America.
39. Shafy, M., *Effect of Low Temperature Aging of Type 316L Austenitic Stainless Weld Metal on Transformation of Ferrite Phase*. Egypt. J. Solids, 2006. **29**(1): p. 151 - 162.
40. Blondeau, R., *Metallurgy and Mechanics of Welding*. 2008: John Wiley and Sons.
41. Schaeffler, A.L., *Constitution diagram for stainless steel weld metal*. Metal Progress, 1949. **56**(11): p. 680 - 680B.
42. Bermejo, A.V., *Predictive and Measurement Methods for Delta Ferrite Determination in Stainless Steels*. Welding Journal, 2012. **91**: p. 113-s 121-s.
43. Delong, W.T., *Ferrite in austenitic stainless steel weld metal*. Welding Journal, 1974. **53**(7): p. 273 - 286.
44. Association, S.C.R.a.T., *The measurement of delta ferrite in cast austenitic stainless steels*, in *Technical bulletin for the of the steel castings research and trade Association*. 1981. p. 4.
45. ASTM, A800/A800M, in *Standard Practice for Steel Casting, Austenitic Alloy, Estimating Ferrite Content Thereof*. 1991, ASTM: West Conshohocken, Pa.
46. Kotecki, D.J. and T.A. Siewert, *WRC-1992 constitution diagram for stainless steel weld metals: a modification of the WRC-1988 diagram*. Welding Journal, 1992. **71**(5): p. 171 - 178.
47. Blondeau, R., *Metallurgy and Mechanics of Welding*. 2008: John Wiley and Sons.
48. Klueh, R.L. and P.J. Maziasz. *Reduced Activation Austenitic Stainless Steels: The Fe-Mn-Cr-C System*. 1988 [cited; 13]. Available from: <http://www.osti.gov/bridge/servlets/purl/7170951-M3Blhg/7170951.pdf>. Last Accessed on May 16, 2012
49. Kotecki, D.J., *Ferrite determination in stainless steel welds : Advances since 1974*. 1997.

50. Lundin, C.D., W. Ruprecht, and G. Zhou, *Ferrite Measurement in Austenitic and Duplex Stainless Steel Castings*. 1999, Department of Energy: Tennessee, Knoxville. p. 1-40.
51. AWS, *ANSI/AWS A4.2-91; Standard procedures for calibrating magnetic instruments to measure the delta ferrite content of austenitic and duplex austenitic-ferritic stainless steel weld metal*. 1991, American Welding Society: Miami, Fla.
52. ISO, *ISO 8249; Welding Determination of Ferrite Number (FN) in austenitic and duplex ferritic-austenitic Cr-Ni stainless steel weld metals*. 2000, ISO: Brussels, Belgium.
53. ASTM, *ASTM E562; Standard practice for determining volume fraction by systematic manual point count*. 1984, ASTM: West Conshohocken, Pa.
54. Davis, J.R. and A.I.H. Committee, *Metals Handbook Desk Edition*. 2 ed. 2008: ASM International.
55. Hall, E.L. and C.L. Briant, *Metall. Trans. A.*, 1984. **A(15)**: p. 793 - 811.
56. Lacombe, P., B. Baroux, and G. Beranger, *Stainless Steels*. Les Editions de Physiques, 1993.
57. Shimada, M., et al., *Acta Mater.*, 2002. **50**: p. 2331 - 2341.
58. Too, C.H., *Sensitisation of Austenitic Stainless Steels*, in *Materials Science and Metallurgy*. August 2002, University of Cambridge: Cambridge. p. 2-5.
59. Reidrich, G. and F. Loib, *Embrittlement of high chromium steels within temperature range of 570-1100 F*. *Arch. Eisenhüttenwes*, Oct 1941. **15**: p. 175 - 182.
60. Newell, H.D., *Properties and Characteristics of 27 % Chromium Iron*. *Met.Prog.*, 1946. **49**: p. 977 - 1028.
61. Heger, J.J., *885 F Embrittlement of the Ferritic Chromium-Iron Alloys*. *Met.Prog.*, 1951. **60**: p. 55 - 61.
62. Lena, A.J. and M.F. Hawkes, *475 C (885 F) Embrittlement in Stainless Steels*. *Trans. AIME*, 1954. **200**: p. 607 - 615.
63. Zapffe, C.A., *Fractographic Pattern for 475 C Embrittlement in Stainless Steel*. *Trans. AIME*, 1951. **191**: p. 247 - 248.

64. Fisher, R.M. and e. al., *Identification of the precipitate accompanying 885 F embrittlement in chromium steels*. Trans. AIME, 1953. **197**: p. 690 - 695.
65. Williams, R.O. and H.W. Paxton, *The Nature of Aging of Iron-Chromium Alloys Around 500 °C*. J. Iron Steel Inst., 1957. **185**: p. 358 - 374.
66. Blackburn, M.J. and J. Nutting, *Metallography of an iron-21% Chromium Alloy Subjected to 475 °C Embrittlement*. J. Iron Steel Inst., 1964. **202**: p. 610 - 613.
67. Gavriljuk, V.G. and H. Berns, *High Nitrogen Steels: Structure, Properties, Manufacture, Applications*. 1999, Berlin: Springer-Verlag. 378.
68. Hull, F.C., *Effects of composition on embrittlement of austenitic stainless steels*. Welding Journal, 1973. **52**(3): p. 104 - 113.
69. ASTM, *G1 - 03; Standard Practice for Preparing, Cleaning, and Evaluating Corrosion Test Specimens*. 2003, ASTM: West Conshohocken, Pa.
70. ASTM, *G31 - 72 (Reapproved 2004); Standard Practice for Laboratory Immersion Corrosion Testing of Metals*. 2004, ASTM: West Conshohocken, Pa.
71. *EN 10002 - 1; Metallic Materials - Tensile Testing -, in Part 1: Method of Test at Ambient Temperature*. 2001, (CEN) european committee for standardization: Brussels, Belgium.
72. *EN ISO 148 - 1: 2009; Metallic materials -- Charpy pendulum impact test in Part 1: Test Method*. 2009, (CEN) european committee for standardization: Brussels, Belgium.
73. Harris, G., N. Setargew, and D. Willis, *Hot dip coating apparatus*. 2006: United States.
74. Courtesy, A., *ASM Handbook. Cast Stainless Steels. Vol. Volume 1*. 2005: ASM International.